PBMC may be a suitable predictor of the response to treatment with TNF-α blockers.

In conclusion, we have demonstrated that IL-17 gene expression in PBMC of RA patients is higher than those in controls. We speculate that IL-17 might play an important role in the pathogenesis of RA, and that IL-17/TNF-α gene expression ratio in PBMC prior to infliximab or etanercept therapy may predict the response to treatment. Further studies are necessary to clarify the molecular basis of IL-17 action in the pathogenesis of RA and whether IL-17 is a suitable target for the treatment of RA.

## References


1. Arner EC, Pratta MA. Independent effects of interleukin-1 on proteoglycan breakdown, proteoglycan synthesis, and prostaglandin $E_2$ release from cartilage in organ culture. Arthritis Rheum 1989;32:288–97.
2. Arend WP, Dayer J-M. Inhibition of the production and effects of interleukin-1 and tumor necrosis factor α in rheumatoid arthritis. Arthritis Rheum 1995;38:151–60.
3. Van de Loo FAJ, Joosten LAB, van Lent PLEM, Arntz OJ, van den Berg WB. Role of interleukin-1, tumor necrosis factor α, and interleukin-6 in cartilage proteoglycan metabolism and destruction: effect of in situ blocking in murine antigen- and zymosan-induced arthritis. Arthritis Rheum 1995;38:164–72.
4. Shanahan JC, St Clair W. Tumor necrosis factor alpha blockade: a novel therapy for rheumatic disease. Clin Immunol 2002;103:231–42.
5. Nishimoto N, Yoshizaki K, Miyasaka N, Yamamoto K, Kawai S, Takeuchi T, et al. Treatment of rheumatoid arthritis with humanized anti-interleukin-6 receptor antibody: a multicenter, double-blind, placebo-controlled trial. Arthritis Rheum 2004;50:1761–9.
6. Dayer JM, Feige U, Edwards CK 3rd, Burger D. Anti-interleukin-1 therapy in rheumatic diseases. Curr Opin Rheumatol 2001;13:170–6.
7. Yao Z, Painter SL, Fanslow WC, Ulrich D, Macduff BM, Spriggs MK, et al. Human IL-17: a novel cytokine derived from T cells. J Immunol 1995;155:5483–6.
8. Fossiez F, Djossou O, Chomarat P, Flores-Romo L, Ait-Yahia S, Maat C, et al. T cell interleukin-17 induces stromal cells to produce proinflammatory and hematopoietic cytokines. J Exp Med 1996;183:2593–603.
9. Aggarwal S, Gurney AL. IL-17: prototype member of an emerging cytokine family. J Leukoc Biol 2002;71:1.
10. Nakae S, Nambu A, Sudo K, Iwakura Y. Suppression of immune induction of collagen-induced arthritis in IL-17-deficient mice. J Immunol 2003;171:6173–7.
11. Nakae S, Saijo S, Horai R, Sudo K, Mori S, Iwakura Y. IL-17 production from activated T cells is required for the spontaneous development of destructive arthritis in mice deficient in IL-1 receptor antagonist. Proc Natl Acad Sci USA 2003;100:5986–90.
12. Lubberts E, Joosten LA, Oppers B, van den Bersselaar L, Coenen-de Roo CJ, Kolls JK, et al. IL-1-independent role of IL-17 in synovial inflammation and joint destruction during collagen-induced arthritis. J Immunol 2001;167:1004–13.
13. Lubberts E, Koenders MI, Oppers-Walgreen B, van den Bersselaar L, Coenen-de Roo CJ, Joosten LA, et al. Treatment with a neutralizing anti-murine interleukin-17 antibody after the onset of collagen-induced arthritis reduces joint inflammation, cartilage destruction, and bone erosion. Arthritis Rheum 2004;50:650–9.
14. Koenders MI, Lubberts E, Oppers-Walgreen B, van den Bersselaar L, Helsen MM, Di Padova FE, et al. Blocking of interleukin-17 during reactivation of experimental arthritis prevents joint inflammation and bone erosion by decreasing RANKL and interleukin-1. Am J Pathol 2005;167:141–9.
15. Koenders MI, Kolls JK, Oppers-Walgreen B, van den Bersselaar L, Joosten LA, Schurr JR, et al. Interleukin-17 receptor deficiency results in impaired synovial expression of interleukin-1 and matrix metalloproteinases 3, 9, and 13 and prevents cartilage destruction during chronic reactivated streptococcal cell wall-induced arthritis. Arthritis Rheum 2005;52:3239–47.
16. Chabaud M, Durand JM, Miossec P. Human interleukin-17: a T cell-derived proinflammatory cytokine produced by the rheumatoid synovium. Arthritis Rheum 1999;42:963–70.
17. Kotake S, Udagawa N, Takahashi N, Matsuzaki K, Itoh K, Ishiyama S, et al. IL-17 in synovial fluids from patients with rheumatoid arthritis is a potent stimulator of osteoclastogenesis. J Clin Invest 1999;103:1345–52.
18. Ziolkowska M, Koc A, Maslinski W. High levels of IL-17 in rheumatoid arthritis patients: IL-15 triggers in vitro IL-17 production via cyclosporin A-sensitive mechanism. J Immunol 2000;164:2832–8.
19. Chen YF, Jobanputra P, Barton P, Jowett S, Bryan S, Clark W et al. A systematic review of the effectiveness of adalimubub, etanercept and infliximab for the treatment of rheumatoid arthritis in adults and an economic exaluation of their cost-effectiveness. Health Technol Assess 2006;10:1–229.
20. Katz Y, Nadiv O, Beer Y. Interleukin-17 enhances tumor necrosis factor-α induced synthesis of interleukins 1,6, and 8 in skin and synovial fibroblasts: a possible role as a "fine-tuning cytokine" in inflammation processes. Arthritis Rheum 2001;44:2176–84.
21. LeGrand A, Fermor B, Fink C, Pisetsky DS, Weinberg JB, Vail TP, et al. Interleukin-1, tumor necrosis factor alpha, and interleukin-17 synergistically up-regulate nitric oxide and prostaglandin E2 production in explants of human osteoarthritic knee menisci. Arthritis Rheum 2001;44:2078–83.
22. Koenders MI, Lubberts E, van de Loo FA, Oppers-Walgreen B, van den Bersselaar L, Helsen MM, et al. Interleukin-17 acts independently of TNF-alpha under arthritic conditions. J Immunol 2006;176:6262–9.
23. Koenders MI, Joosten LA, van den Berg WB Potential new targets in arthritis therapy: interleukin (IL)-17 and its relation to tumour necrosis factor and IL-1 in experimental arthritis. Ann Rheum Dis 2006;65:29–33.
24. Arnett FC, Edworthy SM, Bloch DA, McShane DJ, Fries JF, Cooper NS, et al. The American Rheumatism Association 1987 revised criteria for the classification of rheumatoid arthritis. Arthritis Rheum 1988;31:315–24.
25. Honorati MC, Bovara M, Facchini A. Contribution of interleukin 17 to human cartilage degradation and synovial inflammation in osteoarthritis. Osteoarthritis Cartilage 2002;10:799–807.
26. Wonq PK, Quinn JM, Sims NA, van Nieuwenhuijze A, Campbell IK, Wicks IP, et al. Interleukin-6 modulates production of T lymphocyte-derived cytokines in antigen-induced arthritis and drives inflammation-induced osteoclastogenesis. Arthritis Rheum 2006;54:158–68.
27. Nishimoto N. Clinical benefits of anti-human IL-6 receptor antibody therapy. Clin Calcium 2007;17:562–8.
28. Mangan PR, Harrington LE, O'Quinn DB, Helms WS, Bullard DC, Elson CO, et al. Transforming growth factor-beta induces development of the T(H)17 lineage. Nature 2006;441:231–4.
29. Hirota K, Hashimoto M, Yoshitomi H, Tanaka S, Nomura T, Yamaguchi T, et al. T cell self-reactivity forms a cytokine milieu for spontaneous development of IL-17+ Th cells that cause autoimmune arthritis. J Exp Med 2007;204:41–7.

30. Bettelli E, Carrier Y, Gao W, Korn T, Strom TB, Oukka M, et al. Reciprocal developmental pathways for the generation of pathogenic effector TH17 and regulatory T cells. Nature 2006;441:235–8.
31. Murphy CA, Langrish CL, Chen Y, Blumenschein W, McClanahan T, Kastelein RA, et al. Divergent pro- and antiinflammatory roles for IL-23 and IL-12 in joint autoimmune inflammation. J Exp Med 2003;198:1951–7.
32. Veldhoen M, Hocking RJ, Atkins CJ, Locksley RM, Stockinger B. TGF beta in the context of an inflammatory cytokine milieu supports de novo differentiation of IL-17 producing T cells. Immunity 2006;24:179–89.
33. Bettelli E, Oukka M, Kuchroo VK. T(H)-17 cells in the circle of immunity and autoimmunity. Nat Immunol 2007;8:345–50.
34. Hirota K, Hashimoto M, Yoshitomi H, Tanaka S, Nomura T, Yamaguchi T, et al. T cell self-reactivity forms a cytokine milieu for spontaneous development of IL-17+ Th cells that cause autoimmune arthritis. J Exp Med 2007;204:41–7.
35. Gaffo A, Saag KG, Curtis JR. Treatment of rheumatoid arthritis. Am J Health Syst Pharm 2006;63:2451–65.
36. Mitoma H, Horiuchi T, Hatta N, Tsukamoto H, Harashima S, Kikuchi Y, et al. Infliximab induces potent anti-inflammatory responses by outside-to-inside signals through transmembrane TNF-α. Gastroenterology 2005;128:376–92.

Reprinted From

# The NEW ENGLAND JOURNAL of MEDICINE

VOL. 357 NO. 26

ESTABLISHED IN 1812 DECEMBER 27, 2007 WWW.NEJM.ORG

# Multiple Autoimmune Diseases after Autologous Stem-Cell Transplantation

TO THE EDITOR: Hematopoietic stem-cell transplantation can be an effective treatment in patients with refractory systemic sclerosis.[1] We report on a 19-year-old woman with systemic sclerosis who underwent CD34+-selected autologous hematopoietic stem-cell transplantation in March 2001. Before the transplantation, the physical and laboratory findings showed no evidence of any other autoimmune diseases. After written consent was obtained from the patient, CD34+ hematopoietic stem cells were transplanted according to a method used for systemic sclerosis.[1] The dermal sclerosis improved immediately after transplantation, but thrombocytopenia and Graves' disease developed.

In June 2005, the patient was admitted to the hospital because of fever and edema. Blood tests revealed proteinuria (11.4 g per day) and new autoantibodies in the serum (Fig. 1A). On the sixth hospital day, paralysis developed on the left side as the result of a right cerebral infarction. Systemic lupus erythematosus with membranous-type lupus nephritis (Fig. 2) and the antiphospholipid-antibody syndrome were diagnosed; the patient was treated with prednisolone, warfarin, and cyclosporine. She is currently in clinical remission and is back at work.

During the early phases of immune reconstitution, residual lymphocytes undergo proliferation and expansion, a process controlled by regulatory T cells.[2,3] These cells, defined by the phenotype CD4+CD25+FOXP3+, are important in the prevention of autoimmunity. Interleukin-17–producing helper T (Th17) cells may play a role in the induction of autoimmunity.[4,5] In our patient, the level of serum interleukin-17, released mainly by Th17 cells, was elevated at the onset of the systemic lupus (Fig. 1B). Levels of *FOXP3* messenger RNA, a marker of regulatory T cells, were reduced, suggesting a deficiency of such cells (Fig. 1C). The findings in our patient suggest a role of both regulatory T cells and Th17 in the development of systemic lupus.

Toshiyuki Bohgaki, M.D., Ph.D.
Tatsuya Atsumi, M.D., Ph.D.
Takao Koike, M.D., Ph.D.
Hokkaido University Graduate School of Medicine
Sapporo 060-8638, Japan
tbohgaki@uhnres.utoronto.ca

1. Farge D, Passweg J, van Laar JM, et al. Autologous stem cell

**Figure 1 (facing page). Clinical and Laboratory Findings after CD34+-Selected Autologous Hematopoietic Stem-Cell Transplantation.**
Panel A shows the association between clinical events (including the onset of autoimmune thrombocytopenia [AITP], Graves' disease, systemic edema, and cerebral infarction) and changes in titers of each autoantibody. At the onset of edema, a serum sample from the patient contained anti-Sm, anti-Scl70, and anticardiolipin IgG antibodies (IgG-aCL), in addition to anti-DNA autoantibodies and lupus anticoagulant. The solid line indicates the modified Rodnan total skin thickness score (ranging from 0 to 51, with higher values indicating more thickness). Normal ranges for these levels are as follows: anti-Sm, 0 to 5.9 U per milliliter, anti-Scl70, 0 to 18.9 U per milliliter; and IgG-aCL, <1.3 U per milliliter. Panel B shows serum levels of interleukin-17, transforming growth factor $\beta$1 (TGF-$\beta$1), and interleukin-6. Normal ranges for these levels are as follows: TGF-$\beta$1, 30.95 to 38.65 ng per milliliter; interleukin-6, 0.54 to 1.10 ng per milliliter; and interleukin-17, not detected. Panel C shows changes in T cells, including the ratio of interferon-$\gamma$–producing CD4+ T cells (Th1) and interleukin-4–producing CD4+ T cells (Th2) and FOXP3 messenger RNA (mRNA) on peripheral-blood mononuclear cells. The solid squares indicate levels of CD19+ cells, and the circles indicate levels of CD4+CD25+ cells. Normal ranges are as follows: ratio of Th1 to Th2, 7.22 to 47.52; FOXP3 mRNA, 57.10 to 175.19 copies per glyceraldehyde-3-phosphate dehydrogenase (GAPDH) standard; CD19+, 9.24 to 17.01%; and CD4+CD25+, 5.66 to 10.24%. Calculations were made with the JMP statistical software package, version 5.0 (SAS Institute).

*Reprinted from* THE NEW ENGLAND JOURNAL OF MEDICINE
(ISSN 0028-4793) Vol. 357:2734-2736 (December 27, 2007).

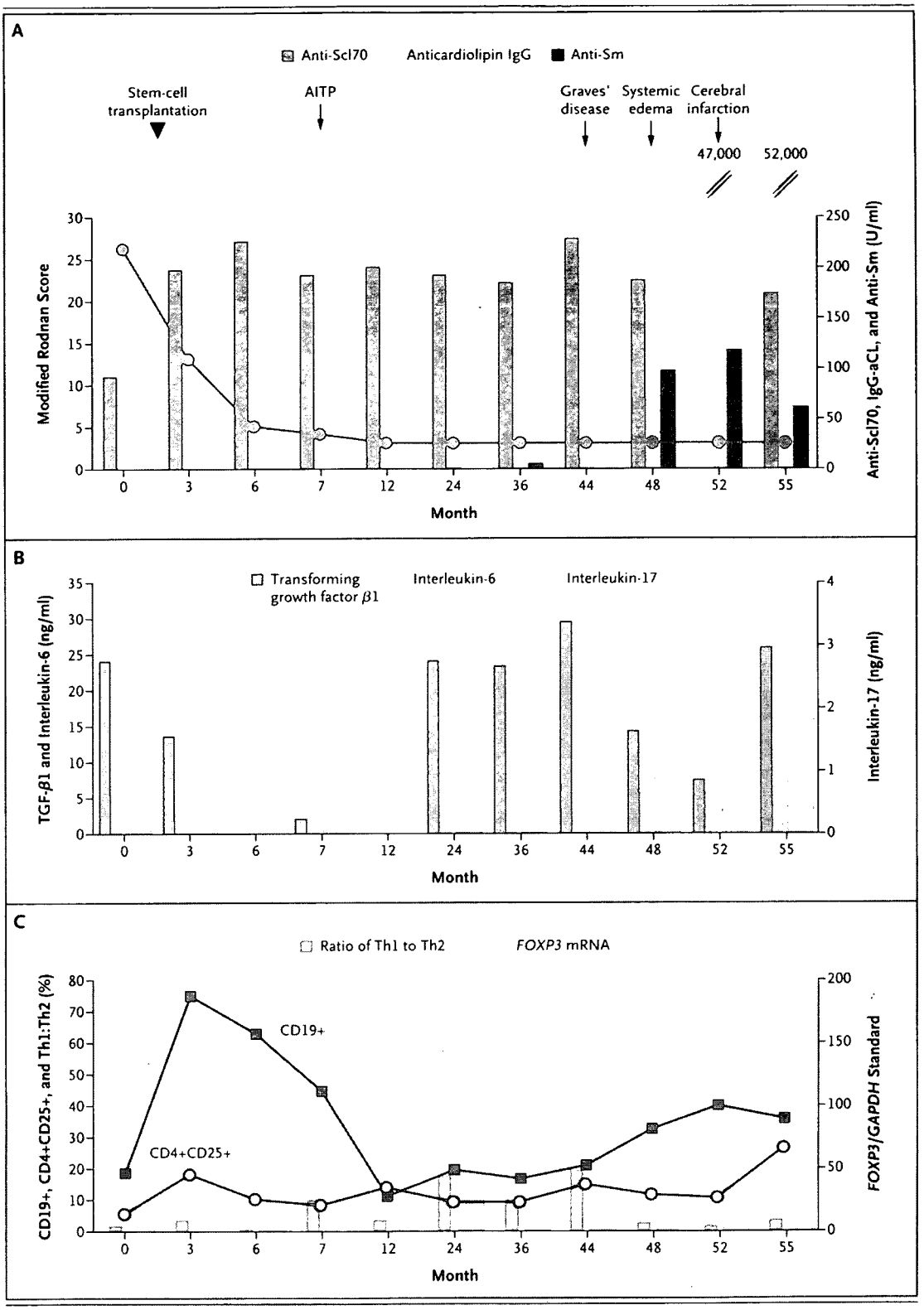
A
Anti-Scl70
Anticardiolipin IgG
Anti-Sm
Stem-cell transplantation
AITP
Graves' disease
Systemic edema
Cerebral infarction
47,000
52,000
Modified Rodnan Score
Anti-Scl70, IgG-aCL, and Anti-Sm (U/ml)
Month
B
Transforming growth factor β1
Interleukin-6
Interleukin-17
TGF-β1 and Interleukin-6 (ng/ml)
Interleukin-17 (ng/ml)
Month
C
Ratio of Th1 to Th2
FOXP3 mRNA
CD19+
CD4+CD25+
CD19+, CD4+CD25+, and Th1:Th2 (%)
FOXP3/GAPDH Standard
Month

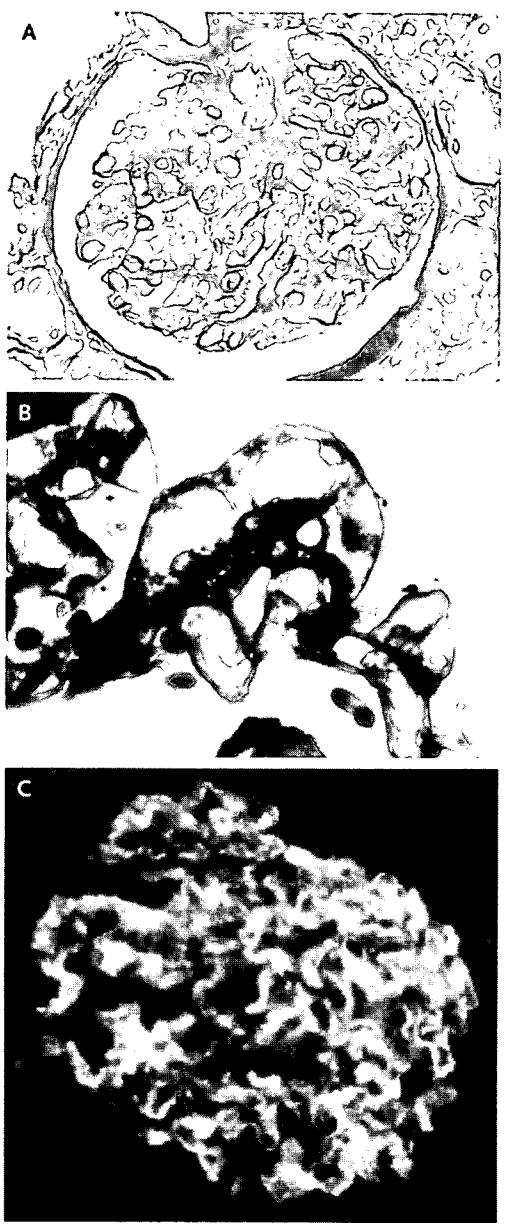


**Figure 2. Renal-Biopsy Specimens Showing Representative Lesions at the Onset of Lupus Nephritis.**

Renal-biopsy specimens show increased mesangial matrix (Panel A, periodic acid–Schiff staining), capillary-wall thickness and bubble appearance (Panel B, periodic acid–methenamine silver staining), and global granular immune deposits (Panel C, immunofluorescence staining).

transplantation in the treatment of systemic sclerosis: report from the EBMT/EULAR Registry. Ann Rheum Dis 2004;63:974-81.

2. de Kleer I, Vastert B, Klein M, et al. Autologous stem cell transplantation for autoimmunity induces immunologic self-tolerance by reprogramming autoreactive T cells and restoring the CD4+CD25+ immune regulatory network. Blood 2006;107:1696-702.

3. King C, Ilic A, Koelsch K, Sarvetnick N. Homeostatic expansion of T cells during immune insufficiency generates autoimmunity. Cell 2004;117:265-77.

4. Bettelli E, Carrier Y, Gao W, et al. Reciprocal developmental pathways for the generation of pathogenic effector TH17 and regulatory T cells. Nature 2006;441:235-8.

5. Bettelli E, Oukka M, Kuchroo VK. T(H)-17 cells in the circle of immunity and autoimmunity. Nat Immunol 2007;8:345-50.

# Melanocortin 2 receptor is required for adrenal gland development, steroidogenesis, and neonatal gluconeogenesis

Dai Chida[a,b,c], Shinichi Nakagawa[d], So Nagai[e], Hiroshi Sagara[f], Harumi Katsumata[g], Toshihiro Imaki[g], Harumi Suzuki[b], Fumiko Mitani[h], Tadashi Ogishima[i], Chikara Shimizu[e], Hayato Kotaki[a], Shigeru Kakuta[a], Katsuko Sudo[a,j], Takao Koike[e], Mitsumasa Kubo[k,l], and Yoichiro Iwakura[a]

[a]Division of Cell Biology, Center for Experimental Medicine, and [f]Fine Morphology Laboratory, Department of Basic Medical Science, Institute of Medical Science, University of Tokyo, 4-6-1, Shirokanedai, Minato-ku, Tokyo 108-8639, Japan; [b]Department of Pathology, Research Institute, International Medical Center of Japan, 1-21-1, Toyama, Shinjuku-ku, Tokyo 162-8655, Japan; [d]Nakagawa Initiative Research Unit, Initiative Research Program, Frontier Research System, RIKEN, 2-1, Hirosawa, Wako, Saitama 351-0198, Japan; [e]Department of Medicine II, Hokkaido University Graduate School of Medicine, Kita 15, Nishi 7, Kita-ku, Sapporo 060-8638, Japan; [g]Department of Bioregulation, Institute of Development and Aging Sciences, Nippon Medical School, 1-396, Kosugi-cho, Nakahara-ku, Kawasaki-city, Kanagawa 211-8533, Japan; [h]Department of Biochemistry and Integrative Medical Biology, School of Medicine, Keio University, 35 Shinanomachi, Shinjuku-ku, Tokyo 160-8582, Japan; [i]Department of Chemistry, Faculty of Sciences, Kyushu University, Hakozaki 6-10-1, Higashi-ku, Fukuoka 812-8581, Japan; [j]Animal Research Center, Tokyo Medical University, 6-1-1, Shinjuku, Shinjuku-ku, Tokyo 160-8402, Japan; and [k]Health Administration Center, Hokkaido University of Education, 5-3-1, Ainosato, Kita-ku, Sapporo 002-8501, Japan

Edited by Richard D. Palmiter, University of Washington School of Medicine, Seattle, WA, and approved September 21, 2007 (received for review July 25, 2007)

**ACTH (i.e., corticotropin) is the principal regulator of the hypothalamus–pituitary–adrenal axis and stimulates steroidogenesis in the adrenal gland via the specific cell-surface melanocortin 2 receptor (MC2R). Here, we generated mice with an inactivation mutation of the MC2R gene to elucidate the roles of MC2R in adrenal development, steroidogenesis, and carbohydrate metabolism. These mice, the last of the knockout (KO) mice to be generated for melanocortin family receptors, provide the opportunity to compare the phenotype of proopiomelanocortin KO mice with that of MC1R–MC5R KO mice. We found that the MC2R KO mutation led to neonatal lethality in three-quarters of the mice, possibly as a result of hypoglycemia. Those surviving to adulthood exhibited macroscopically detectable adrenal glands with markedly atrophied zona fasciculata, whereas the zona glomerulosa and the medulla remained fairly intact. Mutations of MC2R have been reported to be responsible for 25% of familial glucocorticoid deficiency (FGD) cases. Adult MC2R KO mice resembled FGD patients in several aspects, such as undetectable levels of corticosterone despite high levels of ACTH, unresponsiveness to ACTH, and hypoglycemia after prolonged (36 h) fasting. However, MC2R KO mice differ from patients with MC2R-null mutations in several aspects, such as low aldosterone levels and unaltered body length. These results indicate that MC2R is required for postnatal adrenal development and adrenal steroidogenesis and that MC2R KO mice provide a useful animal model by which to study FGD.**

adrenocorticotropic hormone (ACTH) | familial glucocorticoid deficiency (FGD) | hypothalamus–pituitary–adrenal | zona fasciculata

The adrenal gland regulates a number of essential physiological functions in adult organisms through the production of steroids and catecholamines. Maintenance of adrenal structure and function is regulated through the integration of extra- and intracellular signals. The pituitary hormone ACTH (i.e., adrenocorticotropic hormone), which is derived from the proopiomelanocortin (POMC) polypeptide precursor, is the principal regulator that stimulates adrenal glucocorticoid (GC) biosynthesis and secretion via the membrane-bound specific receptor for ACTH, ACTH receptor/melanocortin 2 receptor (MC2R) (1).

It was previously demonstrated that, although POMC knockout (KO) mice are born at the expected Mendelian frequency, three-quarters of POMC KO mice undergo neonatal death. Furthermore, those mice surviving to adulthood exhibit obesity, pigmentation defects, and adrenal insufficiency (2–4). POMC KO mice possess macroscopically detectable adrenal glands that lack normal architecture (2, 4, 5). These results demonstrate the importance of POMC-derived peptides in regulating the hypothalamus–pituitary–adrenal axis and adrenal development.

Familial glucocorticoid deficiency (FGD), or hereditary unresponsiveness to ACTH [Online Mendelian Inheritance in Man (OMIM) no. 202200; www.ncbi.nlm.nih.gov/entrez/dispomim.cgi?id=202200], is an autosomal recessive disorder resulting from resistance to the action of ACTH on the adrenal cortex. Affected individuals are deficient in cortisol and, if untreated, are likely to die as a result of hypoglycemia or overwhelming infection in infancy or childhood (6). Mutations of MC2R are responsible for 25% of FGD cases. Mutations of the MC2R accessory protein MRAP, which plays a role in the trafficking of MC2R from the endoplasmic reticulum to the cell surface, account for 20% of FGD cases (7), and a third locus responsible for FGD has been suggested (8). There has been no animal model for FGD, and MC2R KO mice are likely to become a valuable tool for the pathophysiological investigation of FGD.

To study specifically the roles of MC2R in adrenal gland development, steroidogenesis, and carbohydrate metabolism, we generated mice with an inactivation mutation of the MC2R gene. We demonstrated that disruption of MC2R leads to neonatal lethality in approximately three-quarters of MC2R KO pups, possibly as a result of hypoglycemia. Those surviving to adulthood exhibited macroscopically detectable adrenal glands with markedly atrophied zona fasciculata (zF) and lack of detectable levels of GC and reduced serum concentrations of aldosterone and epinephrine. Those surviving to adulthood exhibited hypoglycemia after prolonged (36 h) fasting as a result of the reduced expression of the genes involved in gluconeogenesis.

Author contributions: D.C., T.K., M.K., and Y.I. designed research; D.C., S. Nakagawa, S. Nagai, H. Sagara, H. Katsumata, T.I., C.S., H. Kotaki, S.K., K.S., and M.K. performed research; H. Suzuki, F.M., and T.O. contributed new reagents/analytic tools; D.C., S. Nakagawa, H. Sagara, T.I., F.M., M.K., and Y.I. analyzed data; and D.C. and M.K. wrote the paper.

The authors declare no conflict of interest.

This article is a PNAS Direct Submission.

Abbreviations: ACTH, adrenocorticotropic hormone; POMC, proopiomelanocortin; GC, glucocorticoid; KO, knockout; FGD, familial glucocorticoid deficiency; zF, zona fasciculata; zG, zona glomerulosa; ME, medulla; TH, tyrosine hydroxylase.

[c]To whom correspondence should be sent at the b address. E-mail: dchida@ri.imcj.go.jp.

[l]Deceased January 21, 2007.

This article contains supporting information online at [illegible] 0706953104/DC1.

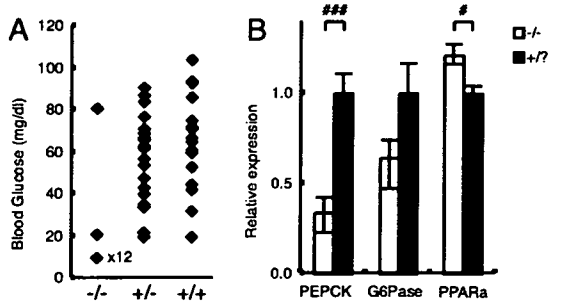


**Fig. 1.** Neonatal hypoglycemia in MC2R KO mice. (*A*) Blood glucose levels on postnatal day 0.5 at 1200 hours. Detection limit was 20 mg/dl. Each point indicates the glucose level of a single pup. The blood glucose level of 12 of 14 homozygous pups was under detection level (<20 mg/dl). The values below detection level were plotted at 10 mg/dl. (*B*) MC2R pups were killed at 1200 hours, and liver RNAs were prepared. The experiments were performed with postnatal day 0.5 $MC2R^{-/-}$ ($n = 6$) and $MC2R^{+/?}$ ($n = 9$) mice. The expression of phospho*enol*pyruvate carboxykinase (PEPCK), glucose-6-phosphatase (G6Pase), and peroxisome proliferator-activated receptor α (PPARa) in the liver was determined by qRT-PCR. Data are expressed as means ± SEM. Statistical significance was determined by *t* test. #, $P < 0.05$.

## Results

**Generation of MC2R KO Mice.** To generate MC2R KO mice, a targeting vector was constructed in which the portion of the MC2R gene encoding the entire coding region (9) was replaced with a neomycin-resistance gene cassette [supporting information (SI) Fig. 7*A*]. One of 545 neomycin-resistant colonies screened was positive as assessed by Southern analysis with an external probe (Fig. 7*B*). Chimeric founder mice were produced from the targeted ES cell clones, and germ-line transmission of the disrupted allele was obtained. MC2R KO mice were backcrossed to C57BL/6J mice for five generations before use in this study. To confirm the deficiency of MC2R, expression of the MC2R gene in the adrenal gland was examined by quantitative real-time PCR (qRT-PCR). No mRNA was detected in $MC2R^{-/-}$ mice, and expression was decreased by approximately half in $MC2R^{+/-}$ mice (Fig. 7*C*).

**Most of the MC2R KO Pups Died Shortly After Birth.** Mice that were homozygous null for MC2R were obtained by interbreeding heterozygous mice. Pups lacking MC2R were born at the expected Mendelian ratio, suggesting that MC2R is not essential for embryonic development. Of 190 mice born from heterozygous MC2R KO parents, 61 pups were dead before weaning at 4 wk of age. Genotype analysis revealed that most of the 61 dead pups were homozygous for the MC2R allele. Genotype analysis of 129 mice at 4 wk revealed 9 homozygote, 74 heterozygote, and 46 WT mice. Approximately three-quarters of MC2R KO pups died before weaning, mostly within 48 h after birth. Most of the mutant newborn mice were indistinguishable from their WT littermates; some homozygous pups were pink and had milk in their stomachs, whereas some homozygous pups were lethargic and pale.

We analyzed blood glucose levels on postnatal day 0.5 at 1200 hours. Three of 57 mice had already died at the time of analysis (two were $MC2R^{-/-}$ and one was $MC2R^{+/-}$). $MC2R^{-/-}$ pups were significantly hypoglycemic compared with $MC2R^{+/?}$ pups (Fig. 1*A*). We found only one of 14 homozygous pups that maintained normal blood glucose levels, comparable with those in WT mice. It is possible that this pup could survive neonatal death and grow to adulthood. Blood glucose levels for 12 of 14 homozygous pups were below detection level (<20 mg/dl). Analysis of blood glucose levels on postnatal day 7 revealed that $MC2R^{-/-}$ pups maintained glucose levels comparable with those of WT mice (data not shown). Expression of phosphoenolpyruvate carboxykinase (PEPCK), a rate-limiting enzyme for gluconeogenesis in liver, was significantly decreased, and expression of glucose-6-phosphatase (G6Pase) was relatively decreased in MC2R KO pups compared with $MC2R^{+/?}$ pups (Fig. 1*B*). The expression of peroxisome proliferator-activated receptor α (PPARα) responsible for β-oxidation of free fatty acids was significantly increased in MC2R KO pups (Fig. 1*B*). These results suggest that MC2R KO mice die as a result of hypoglycemia with decreased gluconeogenesis in the liver and defective neonatal nutritional adaptation. A slight increase in mortality was observed at 3–4 wk of age, due to undetermined cause(s), but no increase in mortality was observed after that period.

The body weights of 12-wk-old MC2R KO mice were indistinguishable from those of their littermates: $MC2R^{-/-}$, 28.7 ± 0.8 g ($n = 4$); and $MC2R^{+/+}$, 28.8 ± 0.6 g ($n = 5$). Whereas FGD patients with MC2R mutations exhibited increased height and POMC KO mice exhibited increased body length (10, 11), MC2R KO mice did not exhibit any significant difference in body length compared with that of their WT siblings: $MC2R^{-/-}$, 9.58 ± 0.17 cm ($n = 5$); and $MC2R^{+/?}$, 9.74 ± 0.07 cm ($n = 10$).

**Adrenal Hypoplasia in MC2R KO Mice That Survived to Adulthood.** In MC2R KO mice, adrenal glands were considerably reduced in size compared with those of their WT siblings: male $MC2R^{-/-}$, 0.58 ± 0.02 mg per pair of glands ($n = 4$); and $MC2R^{+/+}$, 2.24 ± 0.18 mg per pair of glands ($n = 5$). The histological analysis revealed marked hypoplasia of zF in the mutant adrenal gland (Fig. 2*A*). The number of nuclei per 50-μm-wide column in the cortical area, however, was not significantly changed: male $MC2R^{+/-}$, 138.2 ± 13.3; and $MC2R^{-/-}$, 147.7 ± 19.8, $P > 0.35$; and female $MC2R^{+/-}$, 149.7 ± 18; and $MC2R^{-/-}$, 143.8 ± 20.7, $P > 0.61$. These results indicate that the total number of nuclei in the zF was similar in MC2R KO and WT mice. Higher-magnification images revealed that, in the MC2R KO mice, the nuclei in zF were more densely packed with reduced cytoplasmic volume (Fig. 2*B*), suggesting that a decrease in cell size, but not cell number, accounted for the hypoplasia of zF. On the other hand, the zona glomerulosa (zG) and the adrenal medulla (ME) remained fairly intact as shown in the histological sections (Fig. 2*B*). To confirm this idea, we examined the expression patterns of aldosterone synthase cytochrome P450 (P450aldo) and tyrosine hydroxylase (TH), markers for zG and ME, respectively. Both of these markers were similarly expressed in WT and MC2R KO mice (Fig. 2*C*), suggesting that the cells in zG and ME had differentiated into the appropriate cell types. We also noticed that the thickness of capsule was increased in MC2R KO mice (Fig. 2*B*, brackets).

Ultrastructural examination of zF cells in MC2R KO mice revealed that the number of lipid droplets was significantly decreased and mitochondrial appearance was inactive compared with that of WT mice (Fig. 3 *B* and *D*). In contrast, zG cells in MC2R KO mice contained lipid droplets comparable with those in WT mice, and zG cells were not significantly different from those of WT mice (Fig. 3 *A* and *C*). Chromaffin cells in MC2R KO mice exhibited a marked depletion in epinephrine-storing secretory granules (data not shown), and highly vascularized connective tissue was developed in MC2R KO adrenal ME (data not shown). The H&E staining of the adrenal glands of newborn (postnatal day 0.5) MC2R KO mice was not significantly different from that of WT siblings (data not shown), suggesting that postnatal adrenal development was impaired in MC2R KO mice.

**Adrenal Hormones in MC2R KO Mice.** Serum corticosterone levels in MC2R KO mice were undetectable (Fig. 4*A*): male $MC2R^{-/-}$, undetectable ($n = 4$); $MC2R^{+/-}$, 72.0 ± 8.9 ng/ml ($n = 6$); and $MC2R^{+/+}$, 59.0 ± 8.6 ng/ml ($n = 5$). ACTH levels were significantly increased in MC2R KO mice (Fig. 4*B*): male $MC2R^{-/-}$, 1,394 ± 89 pg/ml ($n = 4$); $MC2R^{+/-}$, 370 ± 50 pg/ml ($n = 6$); and $MC2R^{+/+}$,

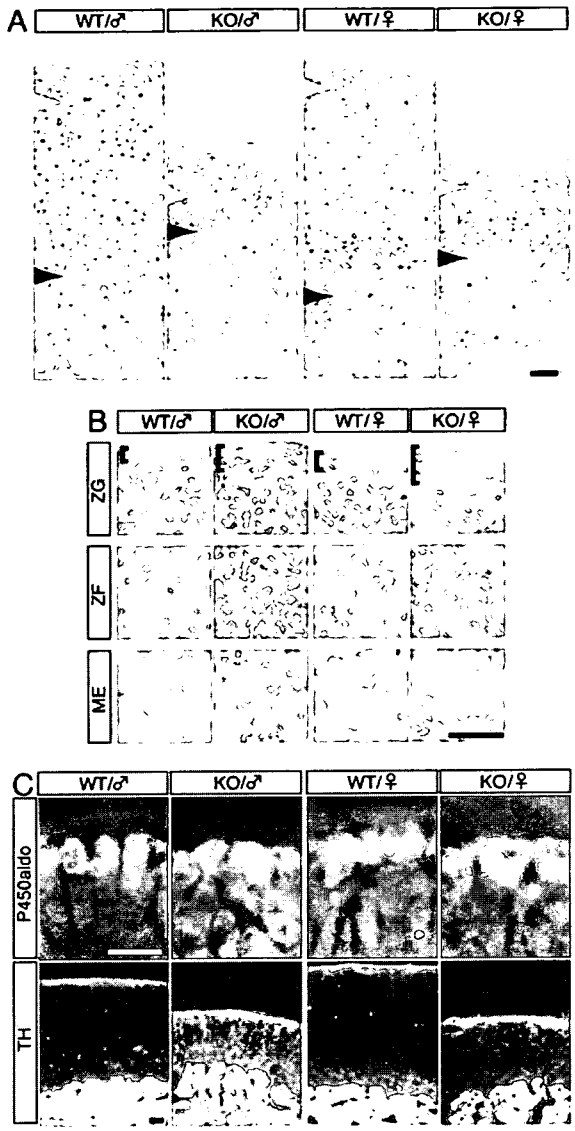


**Fig. 2.** Histological analysis of the adrenal gland of MC2R KO mice. (*A* and *B*) H&E staining of sections from the adrenal gland of WT or MC2R KO mice. Ten-week-old male or 13-wk-old female WT and MC2R KO mice were analyzed. (*B*) Higher-magnification images of zG, zF, and ME shown in *A*. The white and black arrowheads in *A* indicate the border between zG/zF and cortical zone/ME, respectively. The brackets in *B* indicate thickness of the capsule, which was remarkably thicker in the mutant mice. (*C*) Immunofluorescent detection of aldosterone synthase cytochrome P450 (P450aldo) and TH in the adrenal gland of WT and MC2R KO mice. Both enzymes were normally expressed in the mutant mice. (Scale bars, 50 $\mu$m.)

281 ± 106 pg/ml ($n$ = 5). Surprisingly, serum aldosterone levels were significantly decreased in MC2R KO mice (Fig. 4*C*): male $MC2R^{-/-}$, 104 ± 25 pg/ml ($n$ = 4); and $MC2R^{+/+}$, 343 ± 103 pg/ml ($n$ = 5). In this regard, the MC2R-deficient mouse model is different from patients with MC2R-null mutations, in whom there is no mineralocorticoid deficiency and the renin–angiotensin system (RAS) is not affected (OMIM no. 202200). Consistent with the reduced serum corticosterone in MC2R KO mice, thymus and spleen weights were significantly increased and adipose weight was significantly decreased compared with those of WT mice (data not shown).

We analyzed the corticosterone response to exogenously

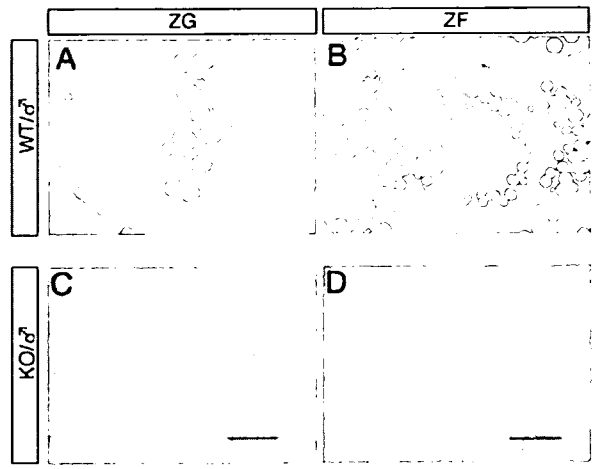


**Fig. 3.** Electron micrographs of the adrenal gland from MC2R KO mice. (*A* and *C*) Electron micrographs of zG of WT or MC2R KO mice. (Scale bars, 2 $\mu$m.) (*B* and *D*) Electron micrographs of zF of WT or MC2R KO mice. (Scale bars, 5 $\mu$m.) Note the remarkable decrease in lipids in zF in MC2R KO mice.

administered ACTH in MC2R KO mice. The responsiveness to ACTH was completely abrogated in MC2R KO mice (Fig. 4*E*): male $MC2R^{-/-}$, ACTH, undetectable ($n$ = 8); $MC2R^{+/-}$, saline, 80.1 ± 13.8 ng/ml ($n$ = 11), and ACTH, 233.9 ± 46.6 ng/ml ($n$ = 11); and $MC2R^{+/+}$, saline, 75.2 ± 20.9 ng/ml ($n$ = 5), and ACTH, 186.9 ± 37.6 ng/ml ($n$ = 8). These results indicate that MC2R is essential for corticosterone release in response to ACTH.

Because ACTH plays an essential role in regulating 11$\beta$-hydroxylase (Cyp11b1) expression, as well as other genes encoding enzymes involved in steroidogenesis (12), we analyzed the expression of adrenal steroidogenic enzymes. Expression levels of cholesterol side-chain cleavage enzyme P450scc (Cyp11a1) (Fig. 5*A*), Cyp21a1 (Fig. 5*B*), and Cyp11b1 (Fig. 5*C*) were significantly reduced in MC2R KO mice, reflecting the hypoplasia of zF. The expression of Cyp11b2 [aldosterone synthase (P450aldo)] was relatively reduced in adrenal glands from MC2R KO mice (Fig. 5*D*). These results collectively indicate that the reduction of corticosterone level (Fig. 4*A*) is due to hypoplasia of zF with reduced lipid droplets (Figs. 2*A* and 3*C*), together with reduced levels of Cyp11b1 and rate-limiting Cyp11a1 (Fig. 5 *A* and *C*).

To determine the physiological effect of reduced aldosterone levels in MC2R KO mice, we measured serum electrolytes and blood pressure at 12 wk of age. There were no differences in the sodium concentrations of MC2R KO and WT mice, whereas chloride levels increased significantly in male MC2R KO mice and tended to increase in female MC2R KO mice (data not shown). Female MC2R KO mice exhibited significantly increased potassium levels (data not shown), whereas male MC2R KO mice did not. Although no significant differences in blood pressure were observed, the heart rate was significantly attenuated in MC2R KO mice (data not shown), consistent with reduced epinephrine levels in MC2R KO mice (Fig. 4*D*). We found that the expression of angiotensin receptor 1b (AT1bR) was significantly increased in MC2R KO mice (Fig. 5*E*), suggesting that renin–angiotensin system (RAS) signaling was enhanced in MC2R KO glomerulosa cells to compensate for the complete absence of ACTH signaling.

Measurement of catecholamine levels demonstrated that epinephrine levels were significantly reduced (Fig. 4*D*): male $MC2R^{-/-}$, 0.12 ± 0.02 ng/ml ($n$ = 4); $MC2R^{+/-}$, 0.72 ± 0.14 ng/ml ($n$ = 6); and $MC2R^{+/+}$, 0.59 ± 0.08 ng/ml ($n$ = 5). However, norepinephrine and dopamine levels were not signif-

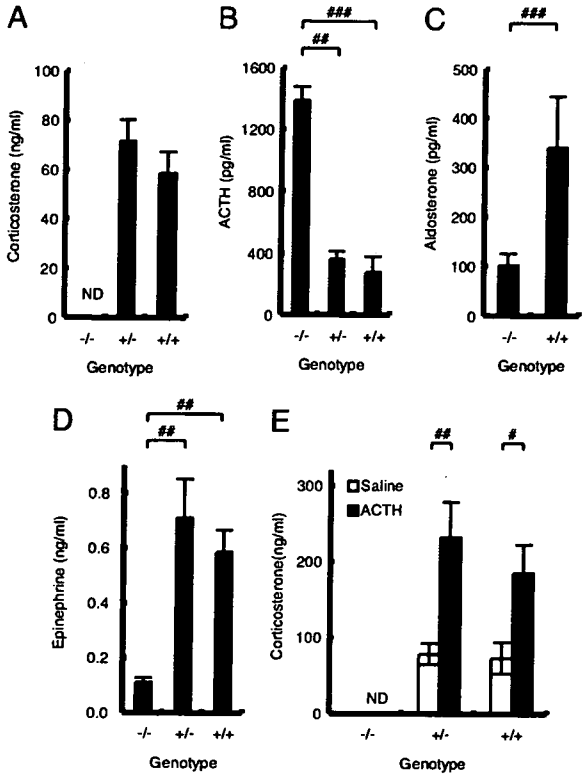


Fig. 4. Hormone levels in MC2R KO mice. (*A–D*) Blood was collected at 1600 hours from male mice (male $MC2R^{-/-}$, $n = 4$; $MC2R^{+/-}$, $n = 6$; and $MC2R^{+/+}$, $n = 5$) fasted for 8 h. Serum corticosterone (*A*), ACTH (*B*), aldosterone (*C*), and epinephrine (*D*) levels were determined. (*E*) Serum corticosterone response after ACTH (10 $\mu$g per kg of body weight) or saline injection in 12-wk-old male $MC2R^{-/-}$ [saline, not determined (ND); ACTH, $n = 8$], $MC2R^{+/-}$ (saline, $n = 11$; ACTH, $n = 11$), or $MC2R^{+/+}$ (saline, $n = 5$; ACTH, $n = 8$) mice. ACTH or saline was injected from 1000 to 1030 hours, and blood was collected after 60 min. Data are expressed as means ± SEM. Statistical significance was determined by one-way ANOVA and Fisher's protected least significant difference (PLSD) test (*A*, *B*, *D*, and *E*) or *t* test (*C*). ###, $P < 0.001$; ##, $P < 0.01$; #, $P < 0.05$.

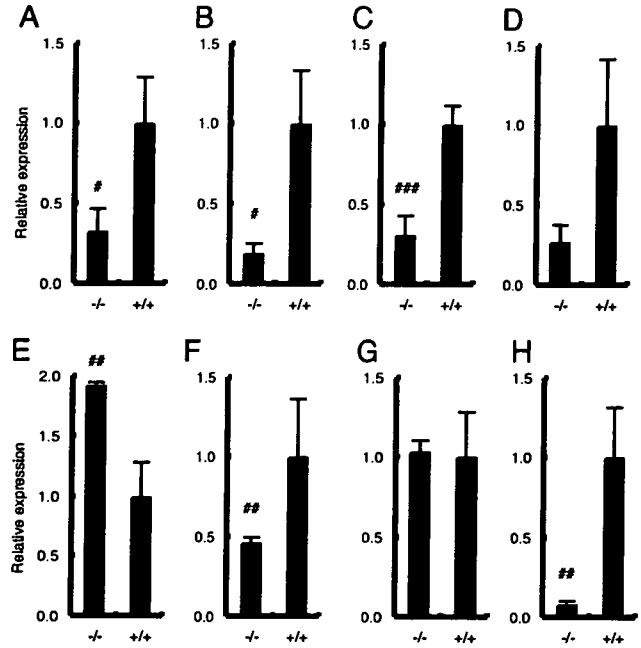


Fig. 5. Adrenal gene expression in MC2R KO mice. Expression of Cyp11a1 (*A*), Cyp21a1 (*B*), Cyp11b1 (*C*), Cyp11b2 (*D*), AT1bR (*E*), TH (*F*), Phox2a (*G*), and phenylethanolamine *N*-methyltransferase (PNMT) (*H*) in adrenal glands from female 12-wk-old $MC2R^{-/-}$ ($n = 4$) and $MC2R^{+/+}$ ($n = 3$) mice was determined by qRT-PCR. Data are expressed as means ± SEM. Statistical significance was determined by *t* test. ###, $P < 0.001$; ##, $P < 0.01$; #, $P < 0.05$.

icantly altered in MC2R KO mice (data not shown). The expression of TH was significantly reduced in MC2R KO adrenal glands (Fig. 5*F*), whereas the expression of Phox2a, a specific marker for chromaffin cells, was not significantly different (Fig. 5*G*), suggesting that MC2R is not required for chromaffin cell development but is necessary for TH expression. These results are consistent with a previous report that GC is not required for chromaffin cell development (13). We also observed that the expression of phenylethanolamine *N*-methyltransferase (PNMT), which catalyzes the conversion of norepinephrine to epinephrine and is modulated by GC, was significantly reduced in adrenal glands from MC2R KO mice (Fig. 5*H*). These results suggest that the reduced epinephrine level in MC2R KO mice is due to the reduced expression levels of PNMT and TH.

**MC2R KO Mice Develop Hypoglycemia upon Prolonged Fasting.** We measured blood glucose levels in animals both fed and fasted for 8 h. Interestingly, adult MC2R KO mice exhibited relatively higher glucose levels than those of WT mice under fed and 8-h fasting conditions. However, the difference was not statistically significant (data not shown). MC2R KO mice exhibited relatively reduced serum insulin levels compared with control littermates. However, the difference was not statistically significant: male $MC2R^{-/-}$, 2,044 ± 190 pg/ml ($n = 4$); and $MC2R^{+/+}$, 2,644 ± 265 pg/ml ($n = 5$).

We next evaluated the role of MC2R during prolonged starvation. After 36 h of starvation, liver gluconeogenesis becomes the major source of blood glucose (14). During a 36-h fast, MC2R KO mice exhibited a faster decline in blood glucose levels (Fig. 6*A*): male $MC2R^{-/-}$, 45.8 ± 11.7 mg/dl ($n = 5$); and $MC2R^{+/+}$, 79.2 ± 9.5 mg/dl ($n = 5$). As anticipated, corticosterone levels in WT mice were increased in response to fasting, whereas corticosterone levels in MC2R KO mice were not increased in response to a 36-h fast (Fig. 6*B*): male $MC2R^{-/-}$, undetectable ($n = 5$); and $MC2R^{+/+}$, 94.4 ± 23.4 ng/ml ($n = 5$). Serum epinephrine was significantly decreased in MC2R KO mice, whereas norepinephrine, dopamine, insulin, and glucagon levels (data not shown) were not significantly different. The expression of PEPCK, which is a rate-limiting enzyme in gluconeogenesis, was significantly decreased, and G6Pase was relatively decreased in MC2R KO mice after a prolonged (36 h) fast (Fig. 6*C*), indicating that the lower blood glucose levels in MC2R KO mice were due to impaired gluconeogenesis.

## Discussion

Immediately after birth, the maternal supply of substrates ceases abruptly, and the newborn mouse has to withstand a brief period of starvation before being fed with milk that is high in fat and low in carbohydrates. The adaptation of neonates to these changes in nutrition and environment requires modification of glucose and fatty acid metabolism, which is controlled by the neonatal increase in glucagon and the fall in insulin (15). Defective gluconeogenesis leads to neonatal death (16). Plasma corticosterone levels are high at delivery and rapidly decline during the first 24 h after birth, and epinephrine and norepinephrine levels are increased severalfold in newborns in response to the stresses of birth, such as transient hypoxia, cold exposure, and cord cutting (15). Because GC plays a critical role in the maintenance of neonatal blood glucose levels through the induction of

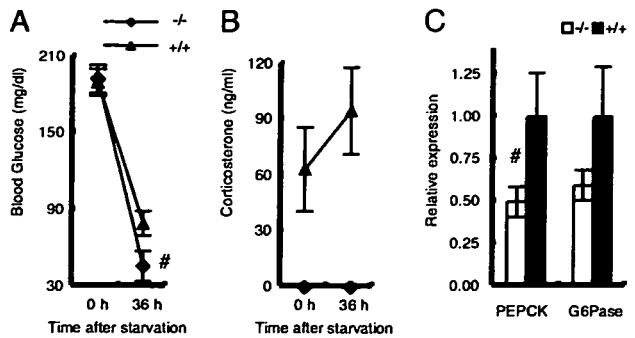


**Fig. 6.** MC2R KO mice develop hypoglycemia during fasting. The experiment was performed with 12-wk-old male MC2R$^{-/-}$ ($n$ = 5) and MC2R$^{+/+}$ ($n$ = 5) mice. (*A* and *B*) At time 0 (2000 hours), food was withdrawn and blood glucose (*A*) and serum corticosterone level (*B*) were measured. After 36 h, mice (at 0800 hours) were killed and serum samples and liver RNA were prepared. Expression of phosphoenolpyruvate carboxykinase (PEPCK) and glucose-6-phosphatase (G6Pase) in the liver was determined by qRT-PCR (*C*). Data are expressed as means ± SEM. The statistical difference was evaluated by two-way ANOVA (factor 1 was genotype and factor 2 was treatment) followed by *t* test to compare the significant difference between the glucose value for 36 h of MC2R KO mice and the glucose value for 36 h of WT mice. #, $P < 0.05$.

gluconeogenesis, one-half of hepatocyte-specific GC receptor KO mice die shortly after birth as a result of hypoglycemia (17). Here, we demonstrated that MC2R KO mice are defective in this adaptation, consistent with a previous report that 75% of POMC KO mice die shortly after birth (2). Genetic replacement of pituitary POMC in POMC KO mice (POMC$^{-/-}$Tg$^{+}$) rescues neonatal lethality in POMC KO mice, suggesting that peripheral POMC, possibly ACTH, is important for neonatal survival (18). These results collectively suggest that ACTH MC2R signaling plays a critical role in the neonatal adaptation to nutrition supply, consistent with the fact that patients with FGD often suffer from neonatal hypoglycemia (OMIM no. 202200) (19). Neonatal hypoglycemia in MC2R KO mice might be secondary to low levels of both circulating corticosterone and epinephrine. It is also interesting that a slight increase in mortality was also observed at 3–4 wk of age because weaning is a crucial period when mice need to adapt to nutritional modifications. In fact, corticosterone concentration is low during the suckling period, increases after 12 days, and peaks at 24 days (15). Further studies are required to clarify the possible role of ACTH MC2R in suckling/weaning adaptation.

We observed significant adrenocortical hypoplasia in adult MC2R KO mice compared with WT siblings. Although zG cells remained fairly intact, zF cells were severely atrophied (Fig. 2), indicating that MC2R is not required for proper development of zG cells but is required for that of zF cells. Adrenal glands of rodents possess a transient zone between the adrenal cortex and the adrenal ME called the murine X zone. The overall function of the X zone remains unclear (20). Detailed studies are required to clarify the possible effect of ACTH deficiency on X zone regression. Because the adrenal glands from MC2R KO pups were indistinguishable in size and histological appearance from those from WT littermates at birth (data not shown), consistent with POMC KO mice (21), the ACTH MC2R signaling pathway regulates postnatal development of the adrenal gland. It was previously proposed that POMC-derived peptides other than ACTH contribute to adrenal development, function, and maintenance. Specifically, cleavage of the N-terminal POMC (amino acids 1–74) results in the generation of shorter peptides with mitogenic properties (22). If POMC-derived peptides other than ACTH have any role in adrenal development, the adrenal phenotype of MC2R KO mice should be less severe than that of POMC KO mice. Compared with the adrenal structure of POMC KO mice previously reported (2, 4), the adrenal structure/morphology of MC2R KO mice was intact, especially in zG. The total number of nuclei in zF of MC2R KO mice was not significantly changed (Fig. 2*A*), suggesting that the proliferation of zF in MC2R KO mice was comparable with that in WT mice. In contrast, it was previously demonstrated that adrenal glands of POMC KO mice on postnatal day 14 had reduced proliferating cell nuclear antigen (PCNA)-positive cells (21). These differences could be explained by the possible role of POMC-derived peptides other than ACTH in adrenal development (22), although we could not exclude the possibility of difference due to genetic background or of compensatory function by other MCRs in the absence of MC2R. Simultaneous comparison of POMC KO mice and MC2R KO mice is required to clarify these possibilities.

We analyzed the adrenal gene expression involved in the syntheses of corticosterone, aldosterone, and catecholamines in MC2R KO mice at 12 wk of age. Two previous studies have shown adrenal gene expression profiles in POMC KO mice. Karpac *et al.* (21) demonstrated that the expression of Cyp11b2, Cyp11b1, and TH in POMC KO mice at 5 wk of age was not significantly different from that in WT mice and suggested that the essential role for POMC peptides is in the maintenance of the adrenal gland and not in differentiation. Coll *et al.* (23) also analyzed the expression of Cyp11b1 and Cyp11a1 and demonstrated that the expression of both was reduced in POMC KO mice at 8 wk of age. Although the latter results were consistent with ours, the former results were not. We could not fully explain the reason for the difference: however, one possible explanation is that adrenal glands of POMC KO and MC2R KO mice at 5 wk of age are indistinguishable from those of WT mice and that they regress thereafter, as suggested by Karpac *et al.* (21). Further developmental studies on the adrenal gland in POMC KO and MC2R KO mice are needed to clarify these issues.

We found that the adrenal glands in MC2R KO mice produce aldosterone at reduced levels, as has been observed in POMC KO mice (2, 4). In this regard, the MC2R-deficient mouse model is different from FGD type 1 patients, who have been reported to exhibit normal serum aldosterone levels (24). This disparity could be explained by the fact that the majority of humans have one or two missense alleles, and homozygous nonsense mutations are very rare. It was recently reported that a small number of such patients may provide biochemical evidence of mineralocorticoid deficiency (25). The role of ACTH in aldosterone production is further supported by the fact that glucocorticoid receptor (GR) KO mice had enlarged adrenal glands with greatly increased expression of not only Cyp11b1 but also Cyp11b2 at embryonic day 18.5 (26). GR KO mice had increased ACTH levels as a result of the deficiency of negative feedback by corticosterone (26). It is possible that increased ACTH levels in GR KO mice are directly responsible for the increased expression of Cyp11b2 in zG. These observations collectively indicate that ACTH MC2R signaling is an important regulator of aldosterone production.

Here we described the initial characterization of MC2R KO mice and confirmed and extended the importance of ACTH-MC2R in neonatal adaptation to nutrition supplies, adrenal development, and the production of corticosterone and aldosterone. The possible role of ACTH-MC2R in adipose metabolism (27), β-cell function (28), and skin homeostasis (29) could be clarified by further analysis of MC2R KO mice.

## Materials and Methods

**Animals.** Generation of MC2R KO mice is described in *SI Materials and Methods*. For analysis of tissue weight, 12-wk-old mice of each genotype were evaluated. Adrenal glands were dissected, cleaned of fat under a stereoscopic microscope, and

weighed. Epididymal white adipose tissue, inguinal white adipose tissue, thymus, and spleen were dissected and weighed. Whole-tissue samples were isolated and placed on saline-saturated filter papers to remain hydrated until weighing. All of the mice were kept under specific pathogen-free conditions in an environmentally controlled clean room in the Laboratory Animal Research Center, Institute of Medical Science, University of Tokyo. The experiments were conducted according to institutional ethical guidelines for animal experiments and safety guidelines for gene manipulation experiments.

**Blood Analysis.** For analysis of basal hormone levels, 12-wk-old adult mice of each genotype were evaluated. After 8 h of fasting, at 1600 hours, mice were anesthetized with diethyl ether, and blood samples were collected rapidly from the heart. Serum electrolyte concentrations were measured by the ion-selective electrode method (SRL, Tokyo, Japan). Serum corticosterone, ACTH, and aldosterone levels were determined by RIA with detection limits of 4.8 ng/ml (Amersham, Little Chalfont, United Kingdom), 5 pg/ml (Mitsubishi, Tokyo, Japan), and 0.05 ng/ml (Aldosterone-RIAKIT II; SRL), respectively. Serum catecholamine levels were determined by HPLC (SRL). Male $MC2R^{+/+}$, $MC2R^{+/-}$, and $MC2R^{-/-}$ mice of 12 wk of age were injected i.p. at 1000 hours with either ACTH (Peptide Institute, Osaka, Japan) at a dose of 10 $\mu$g/kg or saline. Animals were killed by decapitation, and blood was collected after 60 min.

**Blood Pressure Measurement.** Blood pressure and heart rate were measured in conscious mice by the indirect tail-cuff method (BP-98A; Softron, Tokyo, Japan) as described in ref. 30.

**Histology and qRT-PCR Analysis.** Histochemical procedures are described in *SI Materials and Methods*. For determination of relative mRNA concentrations, total adrenal gland or liver RNA, isolated by sepazol, was subjected to reverse transcription by using SuperScript III (Invitrogen, Carlsbad, CA). The cDNA was analyzed by automated fluorescent real-time PCR with SYBR Green (Invitrogen) by using an iCycler iQ (Bio-Rad, Hercules, CA). Ribosomal protein S3 (RPS3) was used as a control. Primer sequences were designed by using Universal ProbeLibrary Assay Design Center (www.roche-applied-science.com/sis/rtpcr/upl/adc.jsp) (Roche Applied Science, Indianapolis, IN) or Primer Bank (http://pga.mgh.harvard.edu/primerbank) (31) as described in *SI Materials and Methods*.

**Statistical Analysis.** All values were calculated as means ± SEM. Comparisons of two groups were analyzed by using Student's *t* test; for comparisons of more than two groups, one- or two-way ANOVA was performed, followed by Fisher's protected least significant difference (PLSD) tests, to analyze statistical differences in each group. In all analyses, a two-tailed probability of <5% (i.e., $P < 0.05$) was considered statistically significant.

We thank all of the members of our laboratory for discussion and help with animal care; Dr. Michael S. Patrick for critical reading of this manuscript; and Dr. Atsushi Miyajima (University of Tokyo), Dr. Hiroshi Takemori (National Institute of Biomedical Innovation, Osaka, Japan), and Kuniaki Mukai (Keio University) for reagents. We express our condolences on Dr. Kubo's sudden death during the preparation of this manuscript. This work was supported by grants from the Ministry of Education, Culture, Sports, Science, and Technology of Japan and the Ministry of Health, Labor, and Welfare of Japan.

1. Dallman MF (1984) *Endocr Res* 10:213–242.
2. Yaswen L, Diehl N, Brennan MB, Hochgeschwender U (1999) *Nat Med* 5:1066–1070.
3. Challis BG, Coll AP, Yeo GS, Pinnock SB, Dickson SL, Thresher RR, Dixon J, Zahn D, Rochford JJ, White A, *et al.* (2004) *Proc Natl Acad Sci USA* 101:4695–4700.
4. Coll AP, Challis BG, Yeo GS, Snell K, Piper SJ, Halsall D, Thresher RR, O'Rahilly S (2004) *Endocrinology* 145:4721–4727.
5. Smart JL, Tolle V, Otero-Corchon V, Low MJ (2007) *Endocrinology* 148:647–659.
6. Clark AJL, Weber A (1998) *Endocr Rev* 19:828–843.
7. Metherell LA, Chapple JP, Cooray S, David A, Becker C, Ruschendorf F, Naville D, Begeot M, Khoo B, Nurnberg P, *et al.* (2005) *Nat Genet* 37:166–170.
8. Genin E, Huebner A, Jaillard C, Faure A, Halaby G, Saka N, Clark AJ, Durand P, Begeot M, Naville D (2002) *Hum Genet* 111:428–434.
9. Shimizu C, Kubo M, Saeki T, Matsumura T, Ishizuka T, Kijima H, Kakinuma M, Koike T (1997) *Gene* 188:17–21.
10. Clark AJ, Cammas FM, Watt A, Kapas S, Weber A (1997) *J Mol Med* 75:394–399.
11. Coll AP, Challis BG, Lopez M, Piper S, Yeo GS, O'Rahilly S (2005) *Diabetes* 54:2269–2276.
12. Miller WL (1988) *Endocr Rev* 9:295–318.
13. Finotto S, Krieglstein K, Schober A, Deimling F, Lindner K, Bruhl B, Beier K, Metz J, Garcia-Arraras JE, Roig-Lopez JL, *et al.* (1999) *Development (Cambridge, UK)* 126:2935–2944.
14. Pilkis SJ, Granner DK (1992) *Annu Rev Physiol* 54:885–909.
15. Girard J, Ferre P, Pegorier JP, Duee PH (1992) *Physiol Rev* 72:507–562.
16. Wang ND, Finegold MJ, Bradley A, Ou CN, Abdelsayed SV, Wilde MD, Taylor LR, Wilson DR, Darlington GJ (1995) *Science* 269:1108–1112.
17. Tronche F, Opherk C, Moriggl R, Kellendonk C, Reimann A, Schwake L, Reichardt HM, Stangl K, Gau D, Hoeflich A, *et al.* (2004) *Genes Dev* 18:492–497.
18. Smart JL, Tolle V, Low MJ (2006) *J Clin Invest* 116:495–505.
19. Clark AJ, Metherell LA, Cheetham ME, Huebner A (2005) *Trends Endocrinol Metab* 16:451–457.
20. Hershkovitz L, Beuschlein F, Klammer S, Krup M, Weinstein Y (2007) *Endocrinology* 148:976–988.
21. Karpac J, Ostwald D, Bui S, Hunnewell P, Shankar M, Hochgeschwender U (2005) *Endocrinology* 146:2555–2562.
22. Estivariz FE, Iturriza F, McLean C, Hope J, Lowry PJ (1982) *Nature* 297:419–422.
23. Coll AP, Fassnacht M, Klammer S, Hahner S, Schulte DM, Piper S, Tung YC, Challis BG, Weinstein Y, Allolio B, *et al.* (2006) *J Endocrinol* 190:515–525.
24. Clark AJ, McLoughlin L, Grossman A (1993) *Lancet* 341:461–462.
25. Lin L, Hindmarsh PC, Metherell LA, Alzyoud M, Al-Ali M, Brain CE, Clark AJ, Dattani MT, Achermann JC (2007) *Clin Endocrinol (Oxford)* 66:205–210.
26. Cole TJ, Blendy JA, Monaghan AP, Krieglstein K, Schmid W, Aguzzi A, Fantuzzi G, Hummler E, Unsicker K, Schutz G (1995) *Genes Dev* 9:1608–1621.
27. Boston BA, Cone RD (1996) *Endocrinology* 137:2043–2050.
28. Genuth S, Lebovitz HE (1965) *Endocrinology* 76:1093–1099.
29. Arck PC, Slominski A, Theoharides TC, Peters EM, Paus R (2006) *J Invest Dermatol* 126:1697–1704.
30. Matsuki T, Isoda K, Horai R, Nakajima A, Aizawa Y, Suzuki K, Ohsuzu F, Iwakura Y (2005) *Circulation* 112:1323–1331.
31. Wang X, Seed B (December 15, 2003) *Nucleic Acids Res* 31, 10.1093/nar/gng154.

# Defective Expression of Ras Guanyl Nucleotide-Releasing Protein 1 in a Subset of Patients with Systemic Lupus Erythematosus[1]

**Shinsuke Yasuda,[2]* Richard L. Stevens,† Tomoko Terada,* Masumi Takeda,* Toko Hashimoto,* Jun Fukae,* Tetsuya Horita,* Hiroshi Kataoka,* Tatsuya Atsumi,* and Takao Koike***

**Dysregulation of Ras guanyl nucleotide-releasing protein 1 (RasGRP1) in mice results in a systemic lupus erythematosus (SLE)-like disorder. We therefore looked for defective isoforms and/or diminished levels of human RasGRP1 in a cohort of SLE patients. PBMCs were collected from twenty healthy individuals and thirty-two patients with SLE. mRNA was isolated and five RasGRP1 cDNAs from each subject were sequenced. T cell lysates from healthy controls and SLE patients also were evaluated for their levels of RasGRP1 protein. The accumulated data led to the identification of 13 new splice variants of the human RasGRP1 gene. Not only did our SLE patients have increased levels and types of these defective transcripts relative to normal individuals, two SLE patients were identified whose PBMCs and T cells contained very little, if any, functional RasGRP1 mRNA and protein. The presence of aberrantly spliced RasGRP1 transcripts also was correlated with lower levels of RasGRP1 protein in the patients' T cells. The lack of the normal isoform of RasGRP1 in some SLE patients and the increased prevalence of defective isoforms of RasGRP1 in others raise the possibility that dysregulation of this signaling protein contributes to the development of autoimmunity in a subset of SLE patients.** *The Journal of Immunology,* **2007, 179: 4890–4900.**

Systemic lupus erythematosus (SLE)[3] is an autoimmune disease of unknown etiology characterized by the presence of high levels of autoantibodies. It has been proposed that a complex interaction of a number of undefined endogenous genes and their products with undefined pathogens and other factors in the environment somehow leads to dysregulation of adaptive immunity in SLE patients. Thus, a major effort has been made to segregate SLE patients into distinct subgroups based on the mechanism of their defects in adaptive immunity.

T cells use the TCR to distinguish self-Ags and foreign Ags and to undergo positive and negative selection in the thymus (1, 2). Positive selection occurs when TCR-derived signals of low intensity result in the activation of Erk-1, a rise in the intracellular levels of active Ras family members, and the activation of numerous transcription factors in the maturing lymphocytes (3). Ras cycles between an inactive GDP-bound form and active GTP-bound form. In T cells, Ras family members (e.g., N-Ras) are activated by ubiquitously expressed guanine nucleotide exchange factors (GEFs) such as Son of sevenless (4, 5) and Vav1 (6) and by the more restricted GEF Ras guanyl nucleotide-releasing protein (RasGRP) 1 (7–10). RasGRP1 is an intracellular signaling protein that contains an N-terminal GEF domain and C-terminal calcium- and diacylglycerol (DAG)/phorbol ester-binding domains (11). Although RasGRP1 was initially identified and cloned from rat brain by Stone and coworkers (12), this intracellular protein is highly expressed in mouse and human T cells and to a lesser extent in B cells. The human RasGRP1 gene is 76.7 kb, contains 17 exons, and normally encodes an ~95-kDa protein of 797 residues.

RasGRP1 resides in the cytoplasm of quiescent T cells. DAG is generated by phospholipase C when T cells are activated via their TCRs. Binding of DAG to the 50-mer protein kinase C1-like domain in the C-terminal half of RasGRP1 causes the transient translocation of the signaling protein to the inner leaflet of the lymphocyte's plasma membrane. Eventually, RasGRP1 moves from the cell surface to the endoplasmic reticulum and Golgi by a down-regulation mechanism that remains to be determined (13–16). Weakly selecting TCR signals depend on RasGRP1 to drive T cell development (17). Overexpression of RasGRP1 in Jurkat T cells enhances TCR-Ras-Erk signaling and results in increased IL-2 expression when these lymphocytes are exposed to calcium ionophore and PMA (7). RasGRP1$^{-/-}$ mice have a block in thymocyte development and diminished numbers of CD4$^+$CD8$^-$ and CD4$^-$CD8$^+$ T cells (8). By contrast, the overexpression of RasGRP1 in mice results in increased numbers of CD4$^-$CD8$^+$ T cells (18). It therefore has been concluded that RasGRP1 participates in the final stages of T cell maturation (8). RasGRP1-null mice have high circulating levels of IgG and IgE and develop a late-onset lymphoproliferative autoimmune syndrome.

*Department of Medicine II, Hokkaido University Graduate School of Medicine, Sapporo, Japan; and †Department of Medicine, Brigham and Women's Hospital and Harvard Medical School, Boston, MA 02115

Received for publication March 29, 2007. Accepted for publication July 27, 2007.

The costs of publication of this article were defrayed in part by the payment of page charges. This article must therefore be hereby marked *advertisement* in accordance with 18 U.S.C. Section 1734 solely to indicate this fact.

[1] This work was supported by the Japanese Ministry of Health, Labor, and Welfare, the Japanese Ministry of Education, Culture, Sports, Science, and Technology, the Japanese Society for the Promotion of Science, and the National Institutes of Health (grant AI-54950).

[2] Address correspondence and reprint requests to Dr. Shinsuke Yasuda, Department of Medicine II, Hokkaido University Graduate School of Medicine, N15 W7, Kita-ku, Sapporo, Japan. E-mail address: syasuda@med.hokudai.ac.jp

[3] Abbreviations used in this paper: SLE, systemic lupus erythematosus; DAG, diacylglycerol; GEF, guanine nucleotide exchange factor; KLH, keyhole limpet hemocyanin; PSL, prednisolone; qPCR, quantitative PCR; RasGRP, Ras guanyl nucleotide-releasing.

The *lag* mouse created by Layer et al. (19) also develops a SLE-like disorder. Young *lag* mice have reduced numbers of mature T cells due to a block in T cell development. Older *lag* mice have elevated levels of autoantibodies and also develop lymphadenopathy and glomerulonephritis. Positional mapping for a disease-associated gene in the *lag* mouse narrowed the responsible region to a 10-cM interval in the telomeric end of the long arm of chromosome 2, which contains the RasGRP1 gene among other genes. Even though the exact mutation is unknown, no functional RasGRP1 protein is present in the *lag* mouse's splenocytes due to defective processing of its precursor transcript.

The human RasGRP1 gene resides on chromosome 15q15 (20). Numerous gene-linkage studies have been conducted on SLE patients, and many candidates have been identified as possible disease-susceptibility genes in these patients. In agreement with the conclusion that SLE is a polygenic disorder influenced by undefined environmental factors, several sites in the human genome were identified by Rao et al. (21) in their multivariate linkage analysis of 101 SLE-affected sib pairs in the United States. One of the sites identified in that study was an undefined gene on chromosome 15q15. Despite the human gene-linkage data and the *lag* mouse data, abnormal isoforms of human RasGRP1 have not been described. Nevertheless, RasGRP1 acts downstream of the TCR and BCR in lymphocytes and upstream of N-Ras, and the gene that encodes the related signaling protein RasGRP4 is aberrantly spliced in some mast cells (22–24). We therefore looked for dysregulation of RasGRP1 in patients with different autoimmune diseases. We now describe a unique subset of SLE patients with a common abnormality in the expression of this important signaling protein.

## Materials and Methods

### *Subjects*

Twenty apparently healthy Japanese individuals (four males and 16 females; 30.9 ± 6.2 years old, mean ± S.D.) and 32 unrelated Japanese patients with SLE (five males and 27 females; 32.0 ± 9.9 years old, mean ± S.D.) were studied. All patients in this cohort fulfilled the American College of Rheumatology criteria for SLE (25). Based on the British Isles Lupus Assessment Group scoring system (26), disease activity at the time of analysis of their RasGRP1 transcripts and proteins was 11.2 ± 7.3 (range = 0–28). Mean disease duration was 8.2 years (range = <1 month to 28 years). Twenty-three (72%) of our SLE patients were receiving prednisolone (PSL) when we measured the expression of RasGRP1 mRNA and protein in their PBMCs and T cells. The daily dose of PSL in this treated group was 16.0 ± 14.2 mg/day (mean ± S.D., range = 2.5–60) and was based primarily on the patient's disease activity and overall weight. Six (26%) of our SLE patients on PSL therapy received the additional immunosuppressive agents cyclosporine ($n$ = 2), methotrexate ($n$ = 2), cyclophosphamide ($n$ = 1), and mizoribine ($n$ = 1). The remaining nine (28%) SLE patients were evaluated for the presence of aberrant RasGRP1 isoforms before the initiation of any therapy. Twelve patients with other autoimmune diseases served as autoimmune controls. We did not attempt to age or gender match this control group with our SLE patients. The patients in this autoimmune control group had rheumatoid arthritis ($n$ = 5), polymyositis/dermatomyositis ($n$ = 2), systemic sclerosis ($n$ = 3), and Sjogren's syndrome ($n$ = 2). Our study was approved by the Human Ethics Committee of the Hokkaido University Graduate School of Medicine (Sapporo, Japan), and informed consent was obtained from each subject.

### *Isolation and characterization of novel human RasGRP1 transcripts*

PBMCs were collected from our subjects using Ficoll-Paque PLUS (Amersham Biosciences), and RNA was isolated from the resulting cells using TRIzol (Invitrogen Life Technologies). The PBMC-derived transcripts were then converted into cDNA using reverse transcriptase (Toyobo) and an oligo$(dT)_{12-18}$ primer (Invitrogen Life Technologies). The coding regions of the RasGRP1 cDNAs were amplified by a PCR method using the forward primer 5′-CGCGGCCATGGGCACCCTG-3′ and the reverse primer 5′-CTAAGAACAGTCACCCTGCTCCAT-3′, which correspond to sequences residing at the beginning and end of the coding domain of the normal human RasGRP1 transcript noted at GenBank accession no. NM_005739, respectively. After a heat denaturation step, each of the 30 cycles of the subsequent PCR steps consisted of a 15-s denaturing step at 94°C, a 15-s annealing step at 63°C, and a 2-min extension step at 72°C. The resulting PCR products were electrophoresed in 1.0% agarose gels and visualized. The PCR products were also subcloned into pcDNA3.1 V5-His-TOPO (Invitrogen Life Technologies). Five arbitrarily selected cDNAs from each individual were then sequenced using an ABI PRISM 3130 genetic analyzer (Applied Biosystems) and numerous internal forward and reverse sequencing primers.

The forward primer 5′-AAGGACCTCATCTCCCTGTA-3′ and the reverse primer 5′-AAGTAGGCTGTGATCTCATC-3′ also were used to evaluate the prevalence of the frequently found exon 11 deletion splice variants of the human RasGRP1 transcript in our SLE subjects. To serve as PCR controls in these transcript analyses, the forward primer 5′-GTCAGT GGTGGACCTGACCT-3′ and the reverse primer 5′-TCTTC AAGGGGTCTACATGG-3′ were used to detect and quantitate the GAPDH transcript. For amplification of GAPDH cDNAs, each of the 25 cycles of the subsequent PCR steps consisted of a 15-s denaturing step at 94°C, a 15-s annealing step at 55°C, and a 45-s extension step at 72°C. The RasGRP3-specific primers 5′-CCATGGGATCAAGTGGCCTTG-3′ and 5′-AGTCAGCCATCCTCACCATCCTG-3′ were used to isolate the nucleotide sequence of the transcripts that encode the entire coding domain of normal RasGRP3. The PCR conditions were identical with those used to evaluate RasGRP1 mRNA expression. We also evaluated the full-length CD4 transcripts in our patients' PBMCs using the CD4-specific primers 5′-CACAATGAACCGGGGAG-3′ and 5′-GCCTCAAATGGGGCTAC-3′. In these CD4 transcript analyses, each of the 30 cycles of the PCR consisted of a 15-s denaturing step at 94°C, a 15-s annealing step at 55°C, and a 60-s extension step at 72°C.

To investigate the splice-donor and splice-acceptor sites of exon 11 in the human RasGRP1 gene, the relevant sequence was obtained using genomic DNA from the PBMCs of SLE patient 10, who had an exon 11 deletion in all five of his/her sequenced RasGRP1 cDNAs. The forward intron 10 primer was 5′-CAGATTGAGAATTTCAAATTAT-3′ and the reverse intron 11 primer was 5′-ATACAAAACTGAGCCAGG-3′. The forward primer resides 253 nucleotides from the 3′ end of intron 10 for the detection of the branch point sequence used to the remove this intron.

### *Generation and use of anti-human RasGRP1 Abs in SDS-PAGE immunoblot assays*

Anti-human RasGRP1 Abs were generated against the 18-mer peptide MGTLGKAREAPRKPSHGC that corresponds to the normal protein's N terminus. This peptide was chosen as the Ag because its sequence does not resemble that in human RasGRP2 (i.e., MGTQRLCGRGTOGWPGSS), RasGRP3 (i.e., MGSSGLGKAATLDELLCT), or RasGRP4 (i.e., MNRK DIKRKSHQECSGKA). A basic local alignment search tool (BLAST) protein search also revealed no similar sequence in any other known human protein. Finally, we concluded that Abs directed against the N terminus of RasGRP1 should be more valuable than the Abs directed the protein's C terminus because the latter Abs would not allow us to identify truncated isoforms of this signaling protein in our patients' lymphocytes. Five milligrams of the synthetic peptide were coupled to keyhole limpet hemocyanin (KLH) via its C-terminal cysteine. A New Zealand White rabbit was s.c. injected with the peptide-KLH complex in the presence of CFA for the primary immunization. This was followed by reimmunization of the animal with the peptide-KLH complex in IFA. The resulting Abs were affinity purified using the synthetic immunizing peptide coupled to Sulfo-Link gel (Pierce) via its C-terminal cysteine. Protein blots containing lysates of RasGRP1-expressing HEK-293 cells and a human thymus obtained from Clontech were probed with the Abs in the presence or absence of the immunizing peptide.

T cells were purified from ~10 ml of peripheral blood from each subject using the RosetteSep human T cell enrichment cocktail (StemCell Technologies). The purities of these T cells were routinely >85% as assessed on a FACSCalibur flow cytometer (BD Biosciences) by using a FITC-labeled anti-CD3 Ab (BD Biosciences). A mammalian cell lysis kit (catalog no. MCL1; Sigma-Aldrich) was used to prepare lysates of each preparation of T cells. The protein concentrations of these samples were determined using the bicinchoninic acid protein assay (Pierce). Approximately 3 μg of each cell lysate was subjected to SDS-PAGE. The separated proteins were transferred to immune blot polyvinylidene difluoride membranes (Bio-Rad), and immunoblotting was performed using our rabbit anti-human RasGRP1 Abs and a mouse anti-human β-actin Ab (Sigma-Aldrich) followed by the relevant secondary Abs conjugated to HRP. The Ab-treated blots were developed by using the Immobilon Western chemiluminescent substrate

(Millipore). The densities of the bands that correspond to β-actin and full-length RasGRP1 were then measured using the Quantity One software package (Bio-Rad).

### *Generation of recombinant human RasGRP1 isoforms found in SLE patients*

Constructs encoding human RasGRP1 with or without a C-terminal V5 epitope tag were transfected into the epithelial cell line HEK-293 (line CRL-1573; American Type Culture Collection). This cell line was chosen rather than a T cell line because HEK-293 cells do not express RasGRP1, thereby allowing us to interpret data in an experimental situation without endogenous RasGRP1. The cDNAs that encode full-length RasGRP1 and three abnormal isoforms of the signaling protein identified in our SLE patients (splice variants A, B, and D) were subcloned into a pIRESpuro3 vector (Clontech). Transfections were performed using Lipofectamine 2000 reagent (Invitrogen Life Technologies) according to the manufacturer's instructions. After a 24-h incubation, 5 μg/ml puromycin (Sigma-Aldrich) was added to the culture medium to select for RasGRP1-expressing transfectants. To evaluate the expression of recombinant RasGRP1 at the RNA level, the transfected cells were trypsinized, washed, and sonicated using a Microson ultrasonic cell disruptor (Wakenyaku). Total RNA was extracted from the lysates as described above. cDNAs were generated using the QuantiTect reverse transcription kit (Qiagen), which includes a DNase treatment step to minimize the possible contamination of the RNA samples with construct DNA. As an additional control for construct DNA contamination, PCRs were conducted on these RNA samples treated in the same manner but without reverse transcriptase.

A confirmatory real-time quantitative PCR (qPCR) approach was then used to monitor the levels of the different RasGRP1 transcripts in the transfectants. In these instances, the level of the RasGRP1 transcript was normalized to that of the GAPDH transcript using an ABI Prism 7000 sequence detection system and TaqMan MGB probes specific for RasGRP1 (assay identifier Hs00996723_m1) and GAPDH (assay identifier Hs00266705_1) (Applied Biosystems). We chose a RasGRP1-specific primer set in these qPCRs that generates a DNA fragment derived from exons 12 and 13, because this sequence is present in all of our expression constructs. Thus, the primer set can be used to measure the levels of the transcripts that encode normal RasGRP1 and its three splice variants in the transfectants. Relative quantification was performed using the comparable cycle threshold ($C_T$) method in which $\Delta C_T$ is the level of the RasGRP1 transcript in the RNA sample relative to that of the GAPDH transcript. The difference in the expression of the transcripts that encode normal RasGRP1 and its splice variants was defined in each instance as $\Delta\Delta C_T$ and the changes in mRNA levels were defined by $2^{-\Delta\Delta CT}$.

For protein expression analysis, the cells were washed with PBS and then lysed using the mammalian cell lysis kit (Sigma-Aldrich). The presence of the different isoforms of RasGRP1 in the transfectants at the protein level was evaluated by the SDS-PAGE immunoblot method described above, using our anti-RasGRP1 Abs. In some experiments, the transfectants were placed in Opti-MEM I medium (Invitrogen Life Technologies) supplemented with the proteasome inhibitor MG-132 at 25 μM (Calbiochem). The 10 mM stock solution of MG-132 was dissolved in 100% DMSO. Thus, the final DMSO concentration in the culture medium was 0.25%. After a 15-h incubation, the treated cells were washed with PBS and cell lysates were prepared and analyzed as described above. Transfected HEK293 cells also were exposed for 14 h to 2 μM monensin sodium sulfate (Sigma-Aldrich) in Opti-MEM I medium before lysates of these cells were analyzed for their RasGRP1 protein levels.

A cell-free in vitro transcription:translation assay was performed using the PROTEINscript II T7 kit (Ambion) according to the manufacturer's instruction. Briefly, our pIRESpuro3 vectors encoding the V5-labeled normal full-length hRasGRP1 and its defective splice variants A, B, and D were subjected to the transcription step. The rabbit reticulocyte lysates in the kit were then used to translate the transcripts, which were evaluated by the SDS-PAGE immunoblot assay using anti-V5 Ab (Invitrogen Life Technologies).

### *Expression of IL-2 in stimulated CD4$^+$ T cells*

$CD4^+$ T cells were purified from 10 ml of the peripheral blood of normal individuals and SLE patients using the RosetteSep human $CD4^+$ T cell enrichment cocktail (StemCell Technologies). In each instance, 500,000 purified T cells were suspended in 0.5 ml of RPMI 1640 medium containing 10% FCS and then stimulated by plate-bound anti-CD3 (1 μg/ml) and anti-CD28 (2.5 μg/ml; BD PharMingen) Abs. Purified T cells that were not stimulated with the anti-CD3 and anti-CD28 Abs served as negative controls. After a 3.5-h incubation at 37 °C in a humid chamber, total RNA was prepared from each sample and subjected to real-time qPCR for quantitation of its IL-2 mRNA levels. The TaqMan MGB primer set specific for IL-2 (assay identifier Hs00174114_m1) was used in the qPCR protocol. This experiment was performed two to three times for each individual in a triplicate manner.

### *Statistical analysis*

The $\chi^2$ test with Yates' correction was used to compare the frequencies of the identified RasGRP1 variants in SLE patients vs healthy individuals. Clinical features or other parameters between control individuals and patients or between patients with and without splice variants were compared using Mann-Whitney's $U$ test. $p$ values below 0.05 were considered to be significant.

## Results

### *Identification of 13 novel RasGRP1 transcripts in SLE patients caused by defective splicing of its precursor transcript*

RasGRP1 cDNAs were amplified from each patient's PBMCs by using a RT-PCR approach and primers that correspond to the beginning and end of the coding domain of normal RasGRP1 in human T cells (Fig. 1*A*). For this initial screening analysis, a limited number of patients with other rheumatic diseases also were evaluated for their expression of normal and defective RasGRP1 transcripts (Fig. 1*B*). The 2.4-kb cDNA that encodes the normal isoform of RasGRP1 was found in all healthy individuals, as well as in those patients with non-SLE autoimmune disorders. No abnormal RasGRP1 transcripts were found in the PBMCs of SLE patients 1, 4, or 5. In contrast, SLE patients 2, 6, and 7 contained both normal and abnormal RasGRP1 transcripts. Surprisingly, the normal 2.4-kb RasGRP1 RT-PCR product was below detection in SLE patients 3, 8, and 9. When SLE patient 3 was reanalyzed 16 mo later, his/her PBMCs had predominantly normal RasGRP1 transcripts (Fig. 1*C*). The defect in RasGRP1 expression therefore was variable in SLE patient 3. In contrast, analysis of the PBMCs taken from SLE patients 8 and 9 ~8 mo after the initial analysis of these patients revealed a similar defect in RasGRP1 expression (Fig. 1*C*). Of the two SLE patients who reproducibly had virtually no normal RasGRP1 mRNA in their PBMCs, SLE patient 9 had been treated with PSL before the analysis of his/her PBMCs. However, SLE patient 8 had not been given any therapeutic drug. Thus, the failure to detect appreciable amounts of the normal RasGRP1 isoform in SLE patient 8 was not a therapy-induced abnormality. Disease status was significantly different in SLE patients 3 and 8 between the first and the second evaluations of their PBMCs for RasGRP1 expression. SLE patient 3 was treated with cyclosporine to alleviate his/her thrombocytopenia, whereas SLE patient 8 was treated with prednisolone and cyclophosphamide to alleviate his/her fever, cytopenia, and glomerulonephritis. In contrast, neither disease activity nor treatment had changed in SLE patient 9. As noted in Fig. 1*D*, SLE patients 8 and 9 had only full-length CD4 and RasGRP3 transcripts in their PBMCs. Similar CD4 and RasGRP3 transcript findings were obtained when two normal individuals, two rheumatoid arthritis patients, and SLE patient 4 were analyzed. Thus, the T cells in SLE patients 8 and 9 did not have a global defect in mRNA processing, including the posttranscriptional processing of another RasGRP family member.

Different sized PCR products were detected in many of our SLE patients. Nevertheless, as noted below, RasGRP1 transcripts lacking exon 11 were frequently observed. We therefore next used a PCR approach to amplify exons 10, 11, and 12 in the RasGRP1 transcripts from the same cDNA samples noted in Fig. 1. Nucleotide sequence analysis confirmed that the generated ~500-bp product noted in the *middle panels* of Fig. 1 corresponds to that in normal RasGRP1 transcripts with its three exons, whereas the ~400-bp product corresponds to abnormal RasGRP1 transcripts lacking exon 11. The ~500-bp fragment was prevalent in every

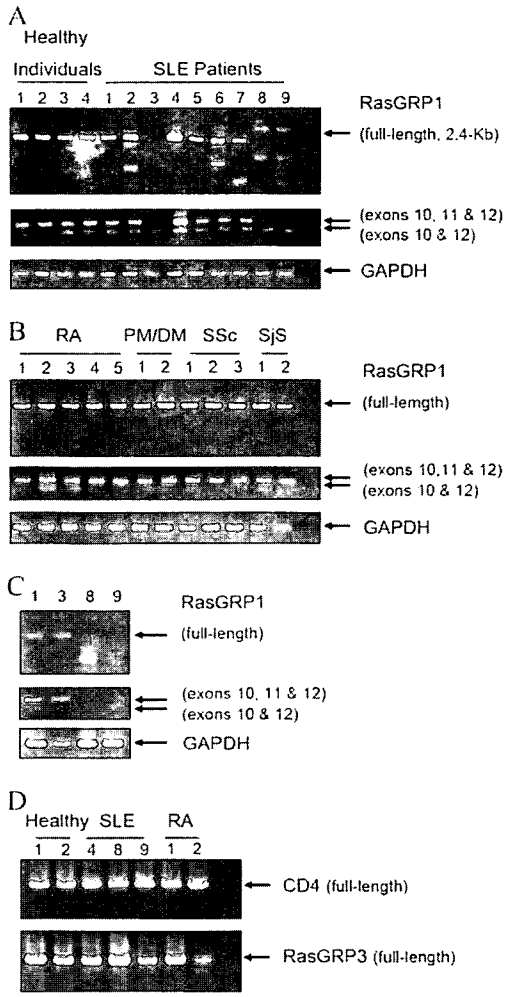


**FIGURE 1.** Identification of normal and defective RasGRP1 transcripts in the PBMCs of healthy individuals, SLE patients, and patients with other autoimmune diseases. *A*, A RT-PCR/gel separation approach using exons 1–17 (*upper panel*) and exons 10–12 (*middle panel*) primer sets in the human RasGRP1 gene was conducted to evaluate transcript expression in the PBMCs isolated from four healthy individuals and nine patients with SLE. *B*, The same screening approach was used to evaluate RasGRP1 transcript expression in five patients with rheumatoid arthritis (RA), two patients with polymyositis (PM) or dermatomyositis (DM), three patients with systemic sclerosis (SSc), and 2 patients with Sjogren's syndrome (SjS). GAPDH-specific primers were used in the *lower panel* as a control to quantitate the levels of the housekeeping transcript in the 25 samples. *C*, Months after the initial analysis of their PBMCs, new samples of PBMCs were obtained from SLE patients 3, 8, and 9. RNA from these new samples were analyzed for the presence of defective RasGRP1 transcripts. The same RNA sample from patient 1 used in the *panel A* experiments was used in the *panel C* experiments as a positive control. *D*, $CD4^-$ and RasGRP3-specific primers were then used to assess the levels and presence of aberrant spliced transcripts that encode these two proteins in the PBMCs isolated from two normal individuals, two RA patients, and SLE patients 4, 8, and 9.

control subject even though lesser amounts of the ~400-bp fragment were also found in these samples. In contrast, the ~400-bp product was prevalent in the same three SLE patients in whom we failed to detect the normal RasGRP1 transcript with the first primer set. Because the data with the exon 10/exon 12 primer set essentially confirmed the data with the exon 1/exon 17 primer set, the RasGRP1 gene is transcribed in all of our SLE patients but its precursor transcript is sometimes aberrantly spliced.

To identify the exons that are preferentially lost in the defective RasGRP1 transcripts in our SLE patients, we next collected samples from age- and sex-matched SLE patients and healthy controls. We then attempted to sequence five arbitrarily subcloned RasGRP1 cDNAs from each individual. Although we were not able to generate any RasGRP1 cDNAs from SLE patients 8 or 9 (Fig. 1*A*), RasGRP1 cDNAs from our other 30 SLE patients were obtained. Thus, we sequenced 100 RasGRP1 cDNAs from 20 healthy individuals and 150 RasGRP1 cDNAs from 30 SLE patients. More than 1,000 sequencing reactions were conducted in this study to understand at the molecular level how the RasGRP1 transcript is aberrantly processed in our cohort of SLE patients. The accumulated data resulted in the identification of 13 new isoforms of human RasGRP1 due to alternate splicing of exons 5–17 in its precursor transcript (Fig. 2). The novel splice variants are as follows deletion of exon 11 (splice variant A, GenBank accession no. AY954625); deletion of exons 11 and 16 (splice variant B, GenBank accession no. AY858556); deletion of exons 11 and 13 (splice variant C, GenBank accession no. AY966005); deletion of exons 11, 15, and 16 (splice variant D, GenBank accession no. AY634315); deletion of exon 11 with insertion of a genomic fragment from intron 16 (splice variant E); deletion of exon 16 (splice variant F); deletion of exons 15 and 16 (splice variant G); insertion of 40 nucleotides from intron 12 between exons 11 and 12 (splice variant H); deletion of exons 11 and 15 (splice variant I); deletion of exons 10 and 11 (splice variant J); deletion of exon 13 (splice variant K); deletion of exon 15 (splice variant L); and deletion of the last 44 nucleotides in exon 5 (splice variant M).

The most prominent abnormal RasGRP1 isoform identified in our SLE patients was splice variant A, which lacks only exon 11. Loss of this exon does not cause a frame-shift abnormality or a premature translation termination codon in the transcript. Nevertheless, many of the other RasGRP1 splice variants identified in our study result in a premature translation termination codon. If translated, splice variants A to M should give rise to C-terminal truncated isoforms of this intracellular signaling protein that contain 173–762 residues rather than the 797 residues of normal RasGRP1. An improperly processed transcript that contains one of the gene's first nine introns also should lead to a nonfunctional protein if translated.

Clone numbers and the percentages of splice variants are indicated in Fig. 2 and Table I. The splice variants A, B, D, and F were frequent abnormal isoforms in our SLE patients; these were even detected in some healthy subjects. In contrast, splice variants C, E, G, H, I, J, K, L, and M were only found in the SLE patients. Moreover, the frequency of any aberrant RasGRP1 isoform was significantly greater in the patient group than the healthy group, even if one does not take into account in this statistical analysis our failure to obtain RasGRP1 cDNAs from SLE patients 8 and 9. We compared the clinical features of those patients who have no abnormal RasGRP1 isoform with those who have at least one splice variant (Table II). The SLE patients who had at least one abnormal RasGRP1 cDNA of five sequenced cDNAs tended to be older and carried the diagnosis longer than those SLE patients that lacked an aberrant RasGRP1 isoform. However, there was no significant correlation between disease activity and the presence of aberrant RasGRP1 isoforms. To evaluate the effect of PSL therapy on the generation of aberrant isoforms of RasGRP1, the presence of at least one abnormal splice variant cDNA of five sequenced cDNAs were evaluated in patients who were analyzed before or during therapy. There was no statistical difference in the frequency of having at least one defective RasGRP1 isoform between the patient groups before and during therapy (Table II). Moreover, SLE patient 8,

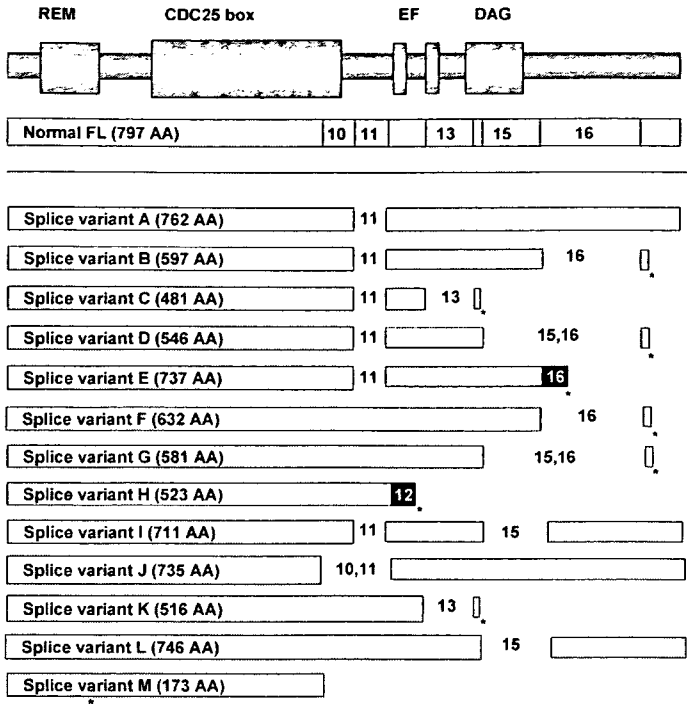


| | healthy (100 clones) | SLE (150 clones) | without vs. with steroid treatment (45 vs. 105 clones) |
|---|---|---|---|
| Splice variant A (762 AA) | 6 (6.0) | 16 (10.7) | 5 vs. 11 |
| Splice variant B (597 AA) | 1 (1.0) | 9 (6.0) | 3 vs. 6 |
| Splice variant C (481 AA) | 0 | 5 (3.3) | 1 vs. 4 |
| Splice variant D (546 AA) | 4 (4.0) | 8 (5.3) | 0 vs. 8 |
| Splice variant E (737 AA) | 0 | 3 (2.0) | 1 vs. 2 |
| Splice variant F (632 AA) | 2 (2.0) | 2 (1.3) | 0 vs. 2 |
| Splice variant G (581 AA) | 0 | 3 (2.0) | 0 vs. 3 |
| Splice variant H (523 AA) | 0 | 2 (1.3) | 0 vs. 2 |
| Splice variant I (711 AA) | 0 | 1 (0.7) | 1 vs. 0 |
| Splice variant J (735 AA) | 0 | 1 (0.7) | 0 vs. 1 |
| Splice variant K (516 AA) | 0 | 1 (0.7) | 0 vs. 1 |
| Splice variant L (746 AA) | 0 | 1 (0.7) | 0 vs. 1 |
| Splice variant M (173 AA) | 0 | 1 (0.7) | 0 vs. 1 |
| | | clones (%) | clones |

**FIGURE 2.** Novel defective RasGRP1 transcripts in the PBMCs of SLE patients. The top panel shows the exon structure and corresponding functional motifs of human RasGRP1, which include the Ras exchange motif (REM), CDC25-like GEF domain (CDC25 box), calcium-binding EF hands, and DAG-binding domain. The exons are not drawn to scale. Splice variants A to M highlighted in the *lower panel* correspond to the 13 new RasGRP1 transcripts identified in our SLE patients. If translated, the number of amino acids (AA) in each expressed isoform is indicated. One hundred RasGRP1-specific cDNAs were isolated and sequenced from 20 healthy individuals. Six, 1, 4, and 2 of these cDNAs corresponded to the splice variants A, B, D, and F, respectively. The remaining 87 cDNAs corresponded to normal, full-length RasGRP1. One hundred and fifty RasGRP1-specific cDNA were isolated and sequenced from 30 SLE patients. The type and number of the identified 58 defective transcripts in these patients are shown whether the SLE patients were on PSL therapy or not. Loss of an exon in the RasGRP1 transcripts that encode splice variants B, C, D, E, F, G, H, K, and M results in a premature translation termination codon (*).

who had no normal RasGRP1 transcripts (Fig. 1), had not been on any therapy before his/her PBMCs were evaluated.

Sequence analysis of a RasGRP1 genomic fragment from a patient who was preferentially expressing RasGRP1 transcripts in his/her PBMCs that lacked exon 11 (e.g., splice variant A) revealed no point mutation from the 3′ end of intron 10 to the 5′ end of intron 11 of his/her RasGRP1 gene. Thus, there is no germline mutation in the intron 10/exon 11 and exon 11/intron 11 splice-sites in either allele of this patient's RasGRP1 gene. The branch point sequence in intron 10, which is used to remove this U2-dependent intron, also was found to be intact in this SLE patient.

*Analysis of RasGRP1 protein levels in T cells*

Rabbit polyclonal Abs were generated against an 18-mer synthetic peptide that corresponds to the unique N terminus of human RasGRP1. The resulting affinity-purified Abs were then used to evaluate RasGRP1 protein levels in the T cells in the peripheral blood of 12 of our 32 SLE patients. The specificity of the preimmune sera, postimmune sera, and affinity-purified anti-RasGRP1 Abs were first evaluated using HEK-293 cells that had been transfected

Table I. *Statistical analysis of aberrant RasGRP1 isoforms in SLE patients and healthy subjects*[a]

| | Percentage (%) | Odds Ratio | 95% CI | *p* Value |
|---|---|---|---|---|
| Loss of exon 11 | | | | |
| Healthy subjects | 11.0 | | | |
| SLE patients | 26.6 | 2.94 | 1.43–6.07 | 0.0129 |
| Lost of any exon | | | | |
| Healthy subjects | 13.0 | | | |
| SLE patients | 36.0 | 3.76 | 1.92–7.37 | 0.0001 |

[a] Odds ratio, confidential interval (CI), and *p* values were calculated by a $\chi^2$ test with Yates' correction to evaluate the significance of the RasGRP1 clones lacking exon 11 or any exon in the cohort of healthy subjects and SLE patients. The percentage (%) of sequenced clones that contained an aberrant RasGRP1 isoform is also indicated. Every healthy subject contained at least one normal RasGRP1 cDNA. In contrast, only abnormal RasGRP1 cDNAs were detected in our analyses of four SLE patients, including patients 8 and 9.

Table II. *Clinical status of SLE patients that contained only normal RasGRP1 transcripts in their PBMCs versus SLE patients with at least one aberrant splice variant of this signaling protein*[a]

| | No Splice Variant | Any Splice Variant | *p* Value |
|---|---|---|---|
| Age (years) | 26.0 ± 6.0 | 36.0 ± 11.0 | 0.024* |
| Male/female | 3/7 | 2/18 | |
| BILAG score | 9.8 ± 5.3 | 11.4 ± 7.0 | 0.494* |
| Disease duration (mo) | 53.8 ± 72.9 | 15.2 ± 11.6 | 0.020* |
| PSL dose (mg/day) | 11.1 ± 15.1 | 12.1 ± 14.2 | 0.790* |
| Patients on therapy | 4 | 3 | |
| Patients on no therapy | 7 | 16 | 0.403† |

[a] The *p* values in the first four rows (*) were calculated using Mann-Whitney's U-test and the *p* value in the last row (†) was calculated by $\chi^2$ test with Yates' correction. BILAG, British Isles Lupus Assessment Group.

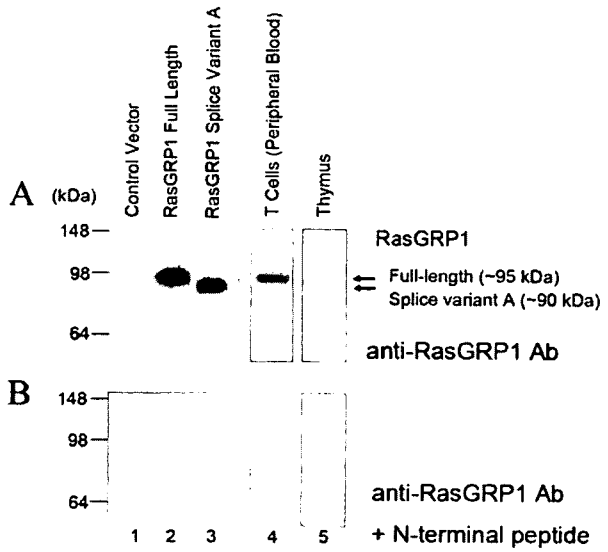


**FIGURE 3.** Generation and evaluation of the specificity of newly created anti-RasGRP1 Abs. Abs were raised in a rabbit against the N-terminal 18-mer amino acid sequence in human RasGRP1. A blot was prepared that contained lysates from HEK-293 cells transfected with vector alone (*lane 1*) or vector containing cDNAs that encode full-length RasGRP1 (*lane 2*) or its truncated splice variant A (*lane 3*). Other protein blots were prepared that contained lysates of peripheral blood T cells (*lane 4* and 5) or the entire thymus (*lane 6*). The resulting blots were probed with the affinity-purified rabbit anti-RasGRP1 Abs in the absence (*A*) or presence (*B*) of the immunizing peptide. Arrows highlight ~95-kDa full-length RasGRP1 and its ~90-kDa splice variant A.

with an expression vector lacking or containing cDNAs that encoded normal RasGRP1 or its abnormal splice variant A. As noted in Fig. 3, no immunoreactive band was detected in lysates of the control transfectants in our SDS-PAGE immunoblot analysis. In contrast, the affinity-purified anti-RasGRP1 Abs recognized the ~95-kDa normal RasGRP1 isoform and its abnormal ~90-kDa splice variant in the transfectants. A nonspecific band of ~64 kDa that could not be blocked by the immunizing peptide was occasionally observed in the T cell lysates from some individuals (data not shown). Nevertheless, our Abs consistently recognized an ~95-kDa protein in lysates of the human thymus and T cells purified from normal peripheral blood (Fig. 3). In all instances, reactivity of the latter band was greatly diminished if the protein blots were reprobed with the anti-RasGRP1 Abs in the presence of the immunizing peptide.

After having established the specificity of our anti-RasGRP1 Abs, we next used them to evaluate the protein levels of varied isoforms of RasGRP1 in T cells purified from the peripheral blood of five healthy individuals and 12 SLE patients (Fig. 4). The RasGRP1 and β-actin protein blot data are shown in Fig. 4, *A* and *B*, respectively. In each instance, the ratio of the density of the RasGRP1 immunoreactive band relative to that of the β-actin immunoreactive band was determined. Density ratios in all healthy controls and in all SLE patients were 0.87 ± 0.05 and 0.64 ± 0.24, respectively, without statistical difference ($p = 0.082$). However, some SLE patients had low levels of RasGRP1 protein, thereby confirming the mRNA data. RasGRP1:β-actin density ratios of individuals without splice variants were significantly higher than those of individuals with any splice variants or whose sequence was not available (0.83 ± 0.16 vs 0.59 ± 0.21, $p = 0.027$) (Fig. 4*C*). Thus, the presence of defective RasGRP1 transcripts in SLE patients generally correlates with the lower levels of normal RasGRP1 protein. Clinical status and information on the sequenced RasGRP1 cDNAs are illustrated in Fig. 4*D* for the individuals whose T cell lysates and RasGRP1 cDNAs were available.

The ability of $CD4^+$ T cells to produce IL-2 after anti-CD3 and anti-CD28 Ab stimulation was evaluated using a real-time qPCR approach (Fig. 4*E*). As previously found by others, the amount of IL-2 mRNA generally increased >10-fold when the peripheral blood T cells from our cohort were stimulated ex vivo via their surface CD3 and CD28 proteins. Although diminished responses were observed in healthy individual 11, the $CD4^+$ T cells isolated from RasGRP1-defective SLE patient 8 barely increased their levels of IL-2 mRNA ($n$ = 2–3).

Despite the presence of transcripts for splice variants A to M in SLE patients, we could not detect appreciable amounts of low m.w. immunoreactive proteins in the T cells of SLE patients using our anti-RasGRP1 Abs. The absence of proteins slightly smaller than normal RasGRP in our patients' T cells that are recognized by our anti-RasGRP1 raised the possibility that splice variants A to M are translated but that many of these newly expressed proteins are rapidly catabolized by an undefined proteolytic pathway to ensure that defective isoforms of the signaling protein do not accumulate in the patient's lymphocytes. An alternate explanation is that some aberrant RasGRP1 transcripts simply are not translated in T cells. To address those possibilities, we next evaluated what happens when cultured HEK-293 cells are transfected with expression constructs that encode the RasGRP1 splice variants A, B, and D. Because an exogenous peptide added at the protein's C terminus might affect the targeting and/or metabolism of these three isoforms of RasGRP1 in the transfectants, additional expression constructs were created to encode recombinant RasGRP1 isoforms that lack epitope tags. We focused on splice variants A, B, and D in this aspect of our study because these abnormal RasGRP1 transcripts are abundant in SLE patients (Fig. 2). Another reason for selecting splice variant D, which lacks exon 15, is because defective splicing of exon 15 in the RasGRP4 transcript occurs in the mast cells of the C3H/HeJ mouse (24).

As assessed by semiquantitative RT-PCR gel analysis (Fig. 5*A*) and by real-time qPCR analysis (Fig. 5*D*), all four stable transfectants contained abundant amounts of the transcript that encodes the relevant RasGRP1 isoform. Due to the loss of exon 11, the RT-PCR products present in the transfectants that had been induced to express splice variants A, B, and D were smaller than the RT-PCR products present in the transfectant that had been induced to express normal RasGRP1 (Fig. 5*A*). At the protein level, the positive control transfectant contained substantial amounts of ~95-kDa RasGRP1. As expected, the transfectants that had been induced to express splice variant A produced a slightly smaller immunoreactive product due to loss of the 35-mer peptide that links the GEF domain to the calcium- and phorbol ester/DAG-binding domains. However, the amount of immunoreactive protein in the latter transfectant was noticeably less than that in the transfectant, which expressed full-length RasGRP1. Surprisingly, no immunoreactive RasGRP1-related protein products were detected in the transfectants that had been induced to express splice variants B or D (Fig. 5*C*), even though their transcripts were abundant (Figs. 5, *A* and *D*). Similar results were obtained when cells were transfected with constructs that encode V5-labeled proteins (data not shown). Thus, our failure to the detect splice variants B and D at the protein level was not due to a technical problem with the anti-RasGRP1 Abs.

To exclude the possibility that the truncated splice variants B and D were preferentially secreted into the condition medium, we next placed cultures of these transfectants overnight in medium supplemented with 2 μM monensin and then performed SDS-PAGE immunoblot analysis on the resulting cell lysates. Because

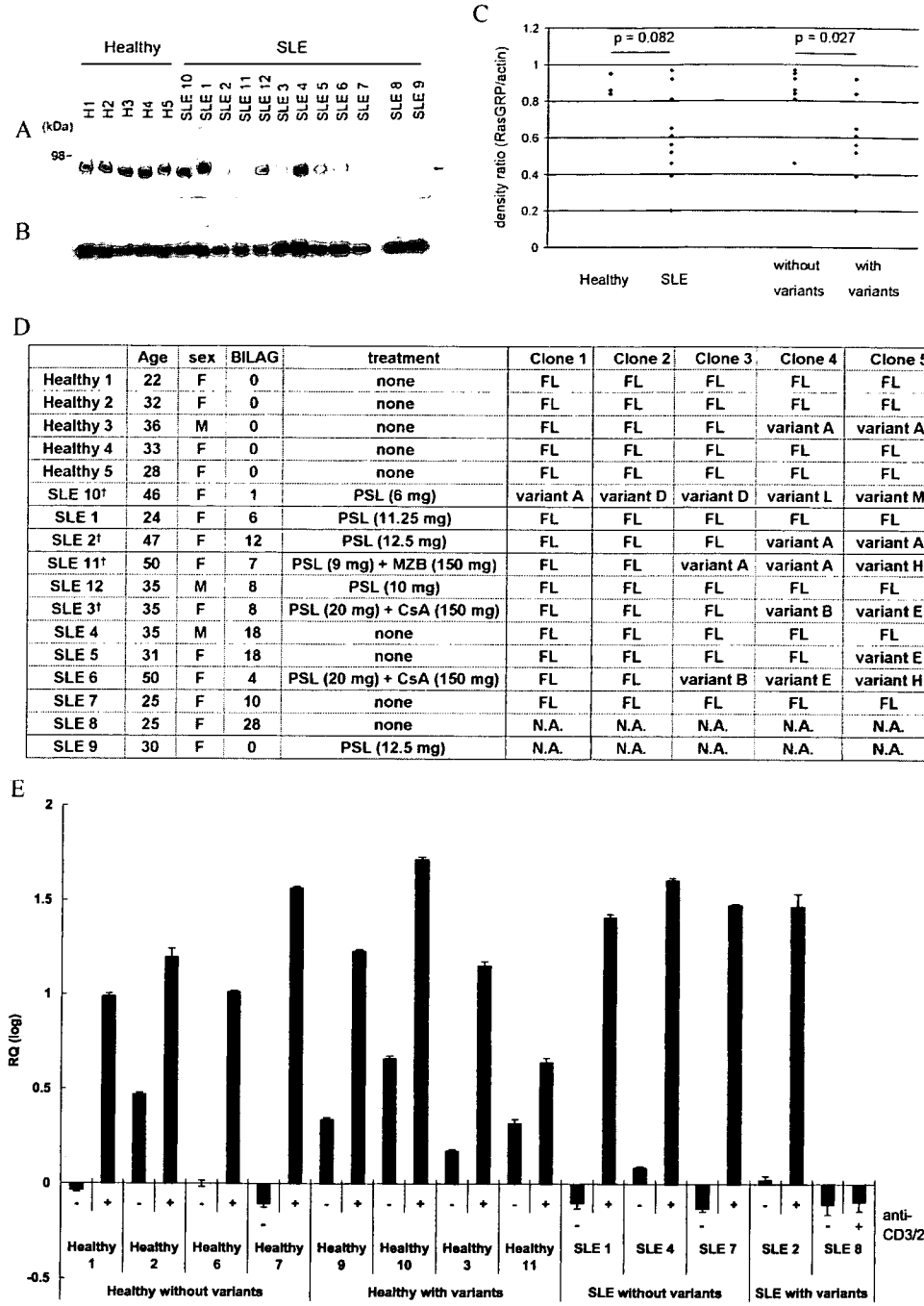


| | Age | sex | BILAG | treatment | Clone 1 | Clone 2 | Clone 3 | Clone 4 | Clone 5 |
|---|---|---|---|---|---|---|---|---|---|
| Healthy 1 | 22 | F | 0 | none | FL | FL | FL | FL | FL |
| Healthy 2 | 32 | F | 0 | none | FL | FL | FL | FL | FL |
| Healthy 3 | 36 | M | 0 | none | FL | FL | FL | variant A | variant A |
| Healthy 4 | 33 | F | 0 | none | FL | FL | FL | FL | FL |
| Healthy 5 | 28 | F | 0 | none | FL | FL | FL | FL | FL |
| SLE 10† | 46 | F | 1 | PSL (6 mg) | variant A | variant D | variant D | variant L | variant M |
| SLE 1 | 24 | F | 6 | PSL (11.25 mg) | FL | FL | FL | FL | FL |
| SLE 2† | 47 | F | 12 | PSL (12.5 mg) | FL | FL | FL | variant A | variant A |
| SLE 11† | 50 | F | 7 | PSL (9 mg) + MZB (150 mg) | FL | FL | variant A | variant A | variant H |
| SLE 12 | 35 | M | 8 | PSL (10 mg) | FL | FL | FL | FL | FL |
| SLE 3† | 35 | F | 8 | PSL (20 mg) + CsA (150 mg) | FL | FL | FL | variant B | variant E |
| SLE 4 | 35 | M | 18 | none | FL | FL | FL | FL | FL |
| SLE 5 | 31 | F | 18 | none | FL | FL | FL | FL | variant E |
| SLE 6 | 50 | F | 4 | PSL (20 mg) + CsA (150 mg) | FL | FL | variant B | variant E | variant H |
| SLE 7 | 25 | F | 10 | none | FL | FL | FL | FL | FL |
| SLE 8 | 25 | F | 28 | none | N.A. | N.A. | N.A. | N.A. | N.A. |
| SLE 9 | 30 | F | 0 | PSL (12.5 mg) | N.A. | N.A. | N.A. | N.A. | N.A. |

**FIGURE 4.** RasGRP1 protein levels in the T cells from healthy individuals and SLE patients. *A–C*, Lysates were prepared from the T cells isolated from five healthy subjects (H1–H5) and from 12 SLE patients (SLE1–SLE12). SLE patients 1–9 in this figure correspond to SLE patients 1–9 in Fig. 1. Approximately 3 $\mu$g of protein from each lysate was subjected to SDS-PAGE. Immunoblotting was performed using anti-RasGRP1 (*A*) and anti-$\beta$-actin (*B*) Abs. In each instance, the density of the bands corresponding to full-length RasGRP1 and $\beta$-actin were measured, and the ratio (RasGRP1/$\beta$-actin) was compared between healthy controls and SLE patients (*C*, *left*) or between individuals without splice variants and with splice variants (*C*, *right*). *D*, The information presented illustrates the clinical status and sequenced RasGRP1 clones of the patients and healthy controls whose peripheral blood T cells were available. For the patients highlighted with the dagger symbol (†) there was a substantial period (>6 mo) between the time when the PBMCs for RNA analysis and the T cells for protein analysis were collected. For patient 9, blood samples for RNA and SDS-PAGE immunoblot analysis of his/her RasGRP1 mRNA and protein were taken on different days within the same month. No RasGRP1 cDNAs were isolated from SLE patients 8 and 9. Thus, the cDNA information is not applicable (N.A.) to these two patients. BILAG, British Isles Lupus Assessment Group score; CsA, cyclosporine; FL, full length; MZB, mizoribine. *E*, CD4$^+$ T cells were incubated in the absence (−) or presence (+) of plate-bound anti-CD3 and anti-CD28 Abs for 3.5 h. The amount of IL-2 mRNA in each sample was then quantitated by real-time qPCR. Shown are the relative quantities (RQ) of GAPDH-corrected levels of the IL-2 transcripts. A nonstimulated sample of a healthy individual without splice variant (Healthy 6) was arbitrary assigned a $2^{-\Delta\Delta CT}$ value of 1. Error bars indicate SE values in this panel.

no immunoreactive protein was detected in the lysates of the monensin-treated cells (data not shown), our failure to detect splice variants B and D inside the transfectants apparently was not due to exocytosis of these defective RasGRP1 isoforms into the conditioned medium. In support of these data, we could not detect immunoreactive RasGRP1 isoforms in the conditioned medium of

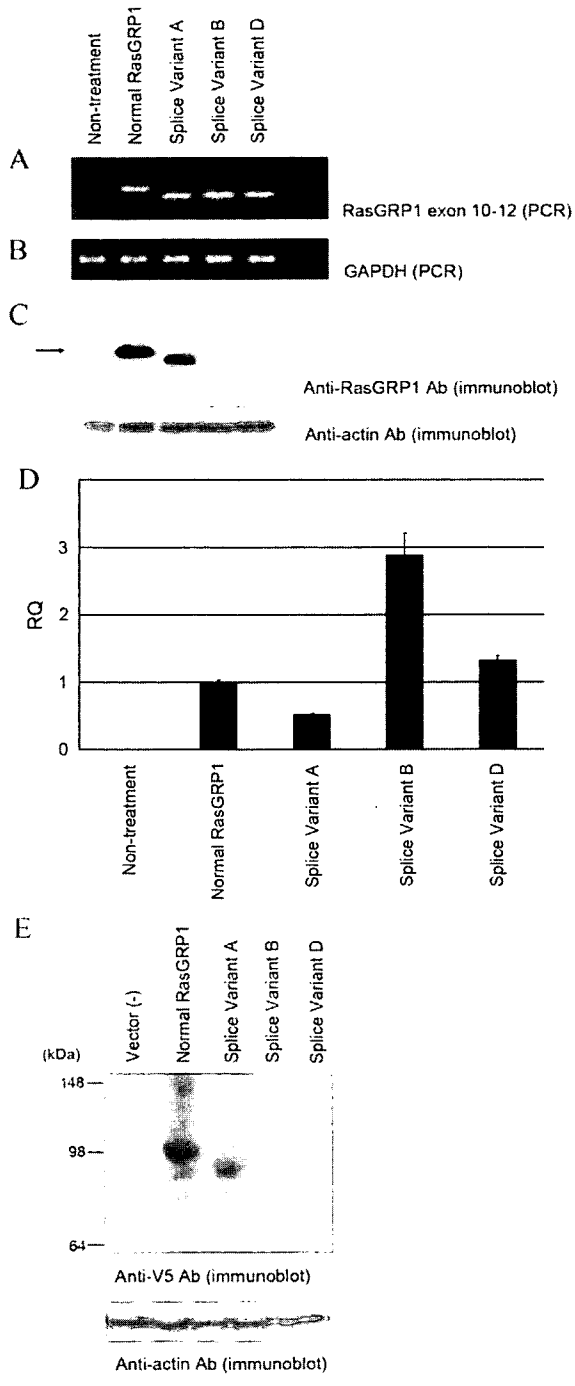


**FIGURE 5.** Expression of recombinant human RasGRP1 in HEK-293 cells. *A–C*, Constructs coding full-length RasGRP1 and its splice variants A, B, and D were expressed in HEK-293 cells. The presence of the relevant RasGRP1 transcript was evaluated in the transfectants using a RT-PCR approach and the exons 10–12 primer set (*A*). The levels of the GAPDH transcript in the five populations of cells were also determined (*B*). Lysates of the transfectants were obtained and subjected to SDS-PAGE immunoblot analysis using anti-RasGRP1 and anti-actin Abs (*C*). The resulting protein blot was probed with our anti-RasGRP1 Abs. The arrow in *C* highlights normal ~95 kDa RasGRP1 that contains 797 amino acids. *D*, A real-time qPCR approach also was used to evaluate RasGRP1 mRNA levels in the negative control cells and the four transfectants. Shown are the GAPDH-corrected levels of the RasGRP1 transcripts in the transfectants that had been induced to express splice variants A, B, and D normalized to that of the positive control transfectant that expresses full-length RasGRP1. The latter was arbitrary assigned a $2^{-\Delta\Delta CT}$ value of 1. Error bars indicate SE values in this panel. RQ, relative quantities. *E*, Cell-free in vitro transcription:translation assays were performed using vectors that encode V5-labeled normal RasGRP1 and its defective splice variants A, B, and D. The resulting products were subjected to immunoblot analysis using anti-V5 Ab (*upper panel*). Actin served as loading control (*lower panel*).

the non-monensin-treated cells that were expressing the splice B and D variants. The levels of immunoreactive RasGRP1 protein in the splice D transfectant also did not increase when these cells were cultured 15 h in the presence of the proteasome inhibitor MG132 (25 $\mu$M) (data not shown). The results obtained from an in vitro translation assay using rabbit reticulocyte lysate are shown in Fig. 5*E*. The normal RasGRP1 transcript and its splice variant A resulted in translated proteins that could be detected with anti-V5 Ab. In contrast, no translated protein was obtained with the splice variant B and D transcripts. The accumulated data suggest that defective splice variants B and D cannot be translated in HEK-293 cells.

## Discussion

RasGRP1 is an intracellular signaling protein essential for the final stages of T cell development (11, 20, 27). Along with RasGRP3 (28–30), RasGRP1 also has been implicated in B cell proliferation and development by facilitating BCR signaling (12). This intracellular GEF functions downstream of the TCR in T cells, downstream of the BCR and Lyn in B cells, and upstream of Ras family members in both cell types. Lyn-null mice develop a SLE-like disorder (31), and decreased expression of Lyn has been reported in some SLE patients (32, 33). A Gly→Asp mutation at residue 13 in N-Ras also causes a human autoimmune lymphoproliferative disorder (34). The accumulated data have led to the conclusion that dysregulation of numerous intracellular proteins that participate in BCR- and/or TCR-dependent signaling pathways in lymphocytes can lead to autoimmune disorders. In regard to our study, loss of RasGRP1 due to targeted ablation of its gene (8) or defective splicing of exon 4 from its precursor transcript (19) causes a lupus-like disorder in mice. Despite the impressive mouse data on the role of RasGRP1 in lymphocyte development and function, no human has been identified with a defect in RasGRP1 expression. Thus, the relevance of the mouse RasGRP1 data to SLE patients remained to be determined. We now describe a subset of SLE patients who preferentially express defective isoforms of RasGRP1 due to aberrant splicing of its precursor transcript.

The 76.7-kb human RasGRP1 gene contains 17 exons, and the proper splicing of its precursor transcript results in an ~5-kb mRNA of which 2.4 kb represents its coding domain. Because microarray assays that simply measure RasGRP1 mRNA levels in a person's lymphocytes cannot be used to identify improperly spliced RasGRP1 transcripts, we used a RT-PCR approach in the initial phase of our study to evaluate the global status of the coding domain of the RasGRP1 transcript in the noncloned PBMCs of healthy individuals, patients with SLE, and patients with other autoimmune disorders. The normal full-length RasGRP1 transcript was abundant in the PBMCs of healthy individuals and our autoimmune control group (Fig. 1). In contrast, two of these initially analyzed SLE patients reproducibly had greatly diminished levels of the normal RasGRP1 transcript in their PBMCs. Additional SLE patients were identified that contained an unusually high level of abnormal RasGRP1 transcripts in addition to the normal RasGRP1 transcript. Analysis of our cDNA sequence data resulted in the identification of 13 new isoforms of human RasGRP1 due to alternate splicing of exons 5–17 in its precursor transcript (Fig. 2). As noted in Fig. 1*A*, SLE patients sometimes had RasGRP1-specific PCR products in their PBMCs that were >2.4 kb in size, suggesting a failure to remove at least one intron in the processed